THE
PHYSICAL REVIEW
A journal of experimental and theoretical physics established by E. L. Nichols in 1893

SECOND SERIES, VOL. 68, NOS. 7 AND 8 OCTOBER 1 AND 15, 1945

Meson Intensity in the Substratosphere

H. J. BHABHA, S. V. CHANDRASHEKHAR AIYA, H. E. HOTEKO, AND R. C. SAXENA
Cosmic Ray Research Unit, Indian Institute of Science, Bangalore, India

(Received July 29, 1945)

The vertical intensities of mesons penetrating 5.25 and 30 cm of lead have been measured to an altitude of 15,000 feet and of those penetrating 20 cm of lead to an altitude of 32,000 feet (275 millibars pressure) by coincidence counter telescopes sent up in an aeroplane from Bangalore, magnetic latitude 3.3°N. A comparison of our results with those of Schein, Jesse, and Wollan indicates that the latitude effect between 3.3°N and 52°N of the vertical intensity of mesons shows no marked increase even to altitudes corresponding to pressures of 275 millibars. This is in striking contrast with the total intensity, which shows a very pronounced increase of latitude effect to these heights.

INTRODUCTION

THE variation with altitude of the total vertical intensity of cosmic rays has been measured by several authors[1–7] at different latitudes using coincidence counter telescopes. The results of such experiments have definitely established the existence of a large latitude effect at high altitudes and are in satisfactory agreement with the deductions of the cascade theory. For brevity we shall call any curve giving the *vertical* intensity of some component or group of cosmic rays as a function of altitude the altitude-intensity curve of that component or group. Valuable information on the processes leading to the creation, annihilation, and scattering of mesons and their dependence on energy could also be obtained through measurements of the altitude-intensity curves of mesons of different energies. There are very few such measurements. Dymond[8] measured the altitude-intensity curve of mesons penetrating 10 cm of lead at Edinburgh, magnetic latitude 59°N, but the work was interrupted by the war and only a preliminary note has been published. Schein, Jesse, and Wollan,[9,10] and Schein, Wollan, and Grötzinger[11] have carried out similar measurements at Chicago, magnetic latitude 52.5°N, using lead absorbers of different thicknesses, and the results of these authors are the only ones available yet. Since cosmic-ray mesons are all produced in the atmosphere, a comparison of the altitude-intensity curves for mesons of different energies *at different latitudes* would give valuable information about the de-

[1] Pfotzer, Zeits. f. Physik **102**, 23 (1936).
[2] T. H. Johnson, Phys. Rev. **54**, 151 (1938).
[3] H. V. Neher and W. H. Pickering, Phys. Rev. **61**, 407 (1942).
[4] R. A. Millikan, H. V. Neher, and W. H. Pickering, Phys. Rev. **63**, 234 (1943).
[5] W. F. G. Swann, G. L. Locher, and W. E. Danforth, Phys. Rev. **51**, 389 (1937).
[6] Carmichael and Dymond, Proc. Roy. Soc. **A171**, 321 (1939).
[7] Regener and Pfotzer, Nature **136**, 718 (1935).
[8] Dymond, Nature **144**, 782 (1939).
[9] M. Schein, W. P. Jesse, and E. O. Wollan, Phys. Rev. **57**, 847 (1940).
[10] M. Schein, W. P. Jesse, and E. O. Wollan, Phys. Rev. **47**, 207 (1935).
[11] M. Schein, E. O. Wollan, and G. Grötzinger, Phys. Rev. **58**, 1027 (1940).

pendence of their creation on the energy of the primary rays. It is therefore important to know the altitude-intensity curves of mesons at different latitudes, and particularly near the geomagnetic equator. No such measurements have been made previously near the geomagnetic equator.

As is well known, India is particularly suited for such measurements. First, the geomagnetic equator passes through south India. Secondly, due to the fact that the magnetic field of the earth is not axially symmetric with regard to its geographic center, India lies in the region of the earth's surface where the cosmic-ray intensity is a minimum, according to the world survey by Millikan and Neher.[12] This means that only the most penetrating cosmic rays can reach the surface of the earth in south India. Even theoretically (cf. Johnson[13]) the critical energy required by a cosmic ray to reach the earth at the magnetic equator in India is over 15×10^9 ev whereas on the equator west of India this critical energy is lower, and reaches the minimum value of 13×10^9 ev in South America. Theoretically the critical energy should reach its maximum value in some region in the Pacific Ocean at about 140°E longitude, that is north of Australia. However, the earth's magnetic field is not that of a pure dipole and it is possible that owing to local variations in the field south India lies in the region where the critical energy is a maximum, as the sea-level survey of Millikan and Neher seems to indicate. In any case, south India lies sufficiently near, if not in, the region of maximum critical energy for a particular importance to attach to measurements made here of the altitude-intensity curves of mesons near the geomagnetic equator.

Vertical intensity measurements if properly carried out are capable of attaining an accuracy sufficient for a quantitative comparison with theory. It is desirable for a proper comparison with theory that in experiments designed to measure the vertical intensity the geometry of the apparatus should be such that the lengths of paths traversed in the atmosphere and the absorber by the different rays measured by it do not differ by more than about 10 percent. Although such a condition tends to reduce the counts per minute, this should be remedied by increasing the number of counters in a tray, and, where possible, by making measurements for a relatively longer period, rather than by reducing the distance between the extreme counters and thus spoiling the geometry, and consequently the accuracy of the measurements. Pfotzer's[1] arrangement for the measurement of the total vertical intensity satisfies this condition but the apparatus used by other workers does not always do so. For example, in the experiments of Neher and Pickering[3] for the measurement of the total vertical intensity, the maximum allowed angle was 47° from the vertical entailing a path length 47 percent greater than that of a vertical particle. Their geometry was further complicated by putting two counters in parallel at a horizontal distance roughly equal to half of the vertical separation of the counters.

It has been shown by Greisen and Nereson[14] that the effect of side showers on counter telescope measurements can be considerable. Since the vertical meson intensity increases much more slowly with altitude than that of the soft component, it is always necessary in measurements of meson intensity to reduce the effect of side showers to a minimum. According to Greisen and Nereson the effect of side showers for a triple coincidence counter telescope is about 14 percent at an altitude 4300 meters and it would be greater at higher altitudes. A quadruple coincidence counter telescope is therefore desirable in measurements of vertical meson intensity which at great heights is only a small fraction of the total intensity.

In order to obtain the maximum information possible from the various experiments it is necessary that the results of different authors should be easily comparable and reproducible. For example, quantitative information about the latitude effect of the different components can only be obtained if this is possible. To this end we suggest that in executing and communicating all future experiments for measuring the variation with altitude of the vertical intensity of cosmic rays of different penetrating power certain criteria be adopted which we indicate below.

[12] R. A. Millikan and H. V. Neher, Phys. Rev. **47**, 207 (1935).
[13] T. H. Johnson, Rev. Mod. Phys. **10**, 193 (1938).
[14] K. Greisen and N. Nereson, Phys. Rev. **62**, 316 (1942).

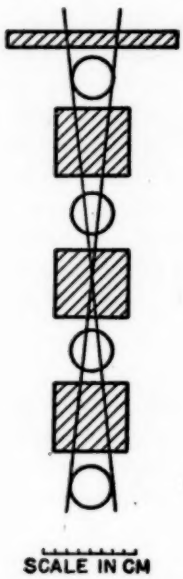

FIG. 1. Arrangement of counters.

The cosmic-ray intensity at any point in the atmosphere is mainly a function of the amount of matter traversed by the rays in reaching that point. Hence comes the importance of measuring the vertical rays only and keeping the variation of path length within about 10 percent by suitably designing the geometry of the apparatus, as we have already mentioned above. Now the pressure is a direct measure of the mass of air traversed by a vertical ray, and it is therefore appropriate that the intensity should be given as a function of pressure rather than in meters of water equivalent, as is often done. It is also what is always measured directly in the experiment. The conversion of pressure into meters of water equivalent involves certain physical assumptions about the relative absorbing powers of air and water and the small uncertainty it introduces is undesirable, especially in view of the fact that the accuracy of cosmic-ray measurements will continually increase in the future. A measurement of pressure in centimeters of mercury is however arbitrary and inconvenient for theoretical purposes. We therefore propose that in the future the intensity be given as a function of pressure measured in *millibars*. Since 1000 millibars, which is equal to the pressure of the standard atmosphere, corresponds to between 10 and 10.3 meters of water equivalent, the pressure in millibars divided by 100 gives immediately to within 3 percent the thickness of the intervening atmosphere in meters of water equivalent. This procedure would therefore have the advantage of communicating what is directly measured in any experiment in a form convenient both for a comparison with theory and with the past experimental results.

It is not the absolute intensities, but the relative values of the intensities which are of significance in comparing the work of different authors. It is therefore essential that the reading at sea level both with and without any absorber that may be used should always be measured with the apparatus concerned and communicated in the paper. Since the latitude effect at sea level and the absorption curve in lead at sea level at different latitudes is known, this would enable a fairly quantitative comparison of the curves of different authors to be made. We would also suggest that the final readings should always be given in a table, even if a graph is included, and the method of averaging the readings and the statistical accuracy be indicated.

We have planned a number of experiments on the basis of the foregoing discussion and carried out a preliminary measurement which is being reported here. In this preliminary experiment, we have measured the variation with height of the intensity of cosmic rays penetrating 20- and 30-cm thick blocks of lead absorbers at Bangalore, magnetic latitude 3.3°N, by sending up quadruple coincidence counter telescopes in an aeroplane. The intensity of mesons penetrating 5.25 cm of lead was also measured by Bhabha's method[15,16] with a triple coincidence counter telescope. Two flights were made, one on December 26, 1944 to an altitude of 15,000 feet and one on December 28, 1944 to an altitude of 32,000 feet. Although further experiments are still in progress, we think that the preliminary results which have already been obtained are of sufficient importance to merit being communicated now.

APPARATUS AND MEASUREMENTS

The counters used in the experiment were filled by a slightly modified form of the procedure

[15] Bhabha, Proc. Ind. Acad. Sci. A19, 23 (1944).
[16] Chandrashekhar Aiya, Proc. Ind. Acad. Sci. A19, 177 (1944).

given by Neher[17] and had a plateau of nearly 300 volts. They were 15 cm long and $1\frac{1}{4}''$–$1\frac{1}{2}''$ in diameter. The distance between the extreme counters was in every case 35 cm. Therefore no single particle making an angle of more than 22° to the vertical could traverse the telescope. Thus a particle recorded at this maximum angle of 22° would only travel a thickness of the atmosphere and absorber 8 percent greater than a particle arriving vertically.

Three distinct sets were used for the measurements. One was designed on the basis of Bhabha's method with a 5.25-cm thick lead absorber which allowed the measurement of the intensity of mesons with energies above 0.93×10^8 ev. It had three counters in a vertical plane working in coincidence with two additional counters in parallel on each side of the middle counter and put in anti-coincidence with the previous three. A lead absorber 1.25 cm thick was inserted below the top counter and a 4.0-cm lead block was put between the middle and bottom counters. A side view of the arrangement is shown to scale in Fig. 1. It has been shown[16] that this splitting of the lead absorber into two parts together with the anti-coincidence arrangement in fact allows the soft component to be cut out by only 5.25 cm of lead and that the two anti-counters to the sides of the middle counter are adequate for reducing the effect of side showers.

FIG. 2. Counter telescope.

[17] Strong and others, *Procedures in Experimental Physics* (Prentice-Hall, Inc., New York, 1938).

The second set had a quadruple coincidence counter telescope with 20 cm of lead as shown in Figs. 2 and 3. In the side view the horizontal lines indicate the active length of each counter. The third set was similar to the second one but had, in addition to the 20 cm of lead, another 10 cm of lead on the top. Each counter telescope, its amplifier, and its plate and bias batteries were all mounted in a box which was closed on all sides and waxed except for a small hole on the top made for the purpose of equalizing the pressure inside and outside the box. Inside each box was an electric heater operated from the aeroplane supply. The high voltage to the counters was supplied from a separate battery box which also had the necessary provision for heating.

The pressure was measured by a standard altimeter. The outside temperature was also measured throughout the flight and was required in order to calculate the real altitude from the indicated altitude. The measurements were made during ascent and descent in both flights. In addition, the airplane flew for half an hour at each "indicated" altitude of 5000, 10,000, 15,000, 20,000, 25,000, and 30,000 feet corresponding to pressures of 832, 671, 530, 430, 332, and 265 millibars, respectively.

The cosmic-ray counts of each of the three sets were recorded on three telephone call counters, and these together with a clock and the altimeter were photographed at the beginning

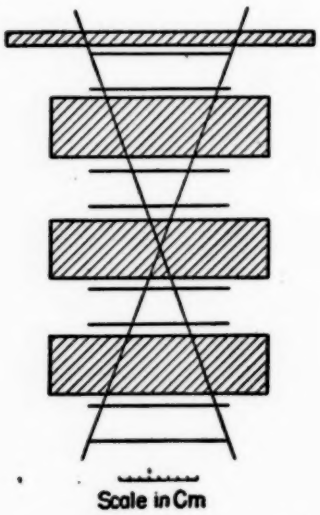

FIG. 3. Counter telescope.

TABLE I. Readings taken on airplane flights.

Indicated altitude in feet	Pressure in cm	Pressure in millibars	Readings with 5.25 cm of lead: counts	time in min.	counts per hr.	Readings with 20 cm of lead: counts	time in min.	counts per hr.	Readings with 30 cm of lead: counts	time in min.	counts/hr.
2900	68.8	906	42	60	42.0± 4.3	36	60	36.0±4.0	24	60	24.0±3.3
5000	63.2	832	22	30	44.0± 6.2	20	30	40.0±6.0	15	30	30.0±5.2
7500	56.4	742	40	38	63.1± 6.3	40	51	47.0±5.0	16	27	35.6±5.9
10000	51.0	671	32	30	64.0± 7.6	20	30	40.0±6.0	17	30	34.0±5.5
12500	45.5	599	60	40	90.0± 7.8	60	59	61.0±5.2	21	28	45.0±6.5
15000	40.3	530	58	31	112.3±10.2	36	31	70.0±6.7	22	31	42.6±6.1
20000	32.7	430				81	47	103.4±7.6			
25000	25.2	332				146	58	148.2±8.2			
30000	20.9	275				274	71	231.5±8.6			

and end of each of these intervals, as also at intermediate points on the way up and down. The results on the way up and down were consistent. No heating was required up to 15,000 feet and the heaters were not put in operation in the first flight. During the second flight two heaters failed to operate, and measurements up to 32,000 feet were obtained only of the intensity of mesons penetrating 20 cm of lead. The readings were consistent on the way up and down, and in good agreement with those made during the first flight. The combined readings of the two flights are given in Table I and plotted in Fig. 4.

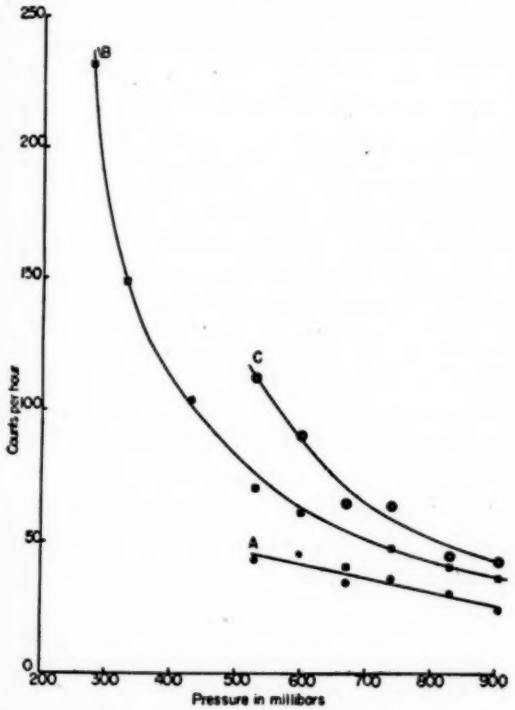

FIG. 4. Curve *A*—Vertical intensity of mesons penetrating 30 cm of lead. Curve *B*—Vertical intensity of mesons penetrating 20 cm of lead. Curve *C*—Vertical intensity of mesons penetrating 5.25 cm of lead. (Note: Since the counters were not of identical diameter in all the three cases, quantitative comparison of the three curves together is not to be made.)

INTENSITY OF MESONS OF DIFFERENT ENERGIES

Certain definite conclusions can be drawn from our results given in Table I and Fig. 4.

1. The intensity of cosmic rays capable of penetrating 30 cm of lead increases very slowly with altitude. The intensity at 15,000 feet (indicated) (530 millibars) is about twice the intensity at 2900 feet (905 millibars).

2. The intensity of mesons capable of penetrating 20 cm of lead also increases slowly with altitude, but at a more rapid rate than in case (1).

3. The intensity of *mesons* capable of penetrating 5.25 cm of lead, i.e., having an energy greater than 0.93×10^8 ev, increases perceptibly more rapidly with altitude. The intensity at 15,000 feet is nearly $2\frac{1}{2}$ times the intensity at 2900 feet.

Schein, Jesse, and Wollan[10] report that there is no difference in the intensity of rays penetrating any absorber thickness between 4 and 18 cm of lead and this appears to contradict the result of Schein, Wollan, and Grotzinger.[11] We are unable to understand the reason for their having found no absorption of rays between 4 and 18 cm of lead contrary to the theoretical expectation and our own experimental results and those of Bostick,[18] Rossi and Greisen,[19] and Hall[20] who find a great increase in the percentage of slow mesons with altitude.

[18] W. H. Bostick, Phys. Rev. **61**, 557 (1942).
[19] B. Rossi and K. Greisen, Phys. Rev. **61**, 121 (1942).
[20] D. B. Hall, Phys. Rev. **66**, 321 (1944).

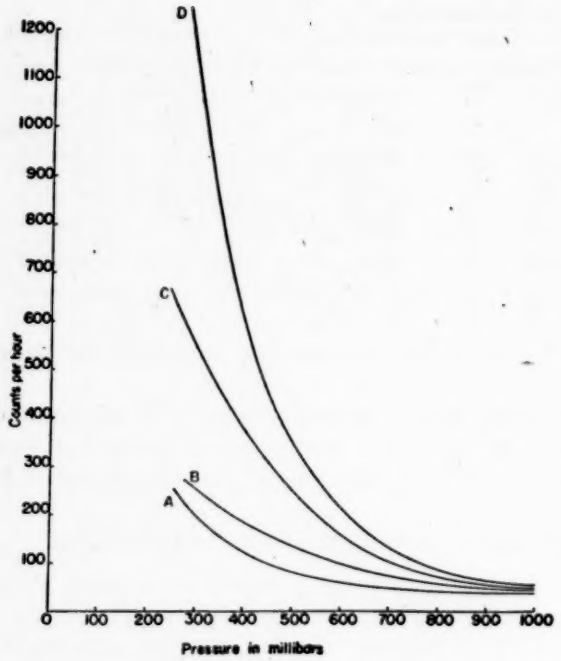

FIG. 5. Curve *A*: Vertical meson intensity at 3.3°N (Bhabha, Aiya, Hoteko and Saxena). Curve *B*: Vertical meson intensity at 52.5°N (Schein, Jesse and Wollan—1941). Curve *C*: Vertical total intensity at 3.3°N (Neher and Pickering). Curve *D*: Vertical total intensity at 49°N (Pfotzer).

It is worth mentioning that our readings at 10,000 feet for all the three apparatuses lie markedly below the three smooth curves drawn through the readings at the other altitudes, but there is not sufficient evidence to decide whether this result is purely a coincidence due to statistical fluctuations or is real.

LATITUDE EFFECT

In Fig. 5 we have plotted our results giving the intensity of mesons penetrating 20 cm of lead at 3.3°N as curve *A* and, for comparison, the latest results of Schein, Jesse, and Wollan[10] for the intensity of mesons at 52.5°N as curve *B*. The two curves have been fitted at sea level to allow for the known latitude and longitude effect[12] of 12 percent. In the same figure, we have plotted as curve *C* the variation of the total vertical intensity with altitude at 3.3°N as given by Neher and Pickering[3] for a triple coincidence counter telescope, this curve being fitted to our curve so as to show a ratio of vertical meson intensity to total vertical intensity of 80 percent as observed at ground level at Bangalore. Curve *D* gives the variation of the total vertical intensity with altitude as measured by Pfotzer[1] at a magnetic latitude of 49°N. The four curves together show at a glance the striking fact that *whereas the latitude effect between 3.3°N and 49°N of the total intensity shows a pronounced increase with altitude, the penetrating component shows practically no such increase of latitude effect even to heights corresponding to pressure of 275 millibars.* The theory of Hamilton, Heitler, and Peng[21] according to which the penetrating component should show only a slightly greater latitude effect than at sea level up to heights corresponding to a pressure of 100 millibars is therefore at least in qualitative agreement with our measurements. The difference in the geometry of the counter telescopes used by the different authors and the statistical accuracy of the results do not yet permit a quantitative comparison.

ACKNOWLEDGMENT

It is with pleasure that we express our great gratitude to Col. M. C. Robinson, Commanding Officer of the 84th Air Depot of the U. S. A. Air Force for giving the permission for the flight. We also wish to express our appreciation to the officers and men under his command who collaborated in the flight, and in particular to the engineering officer Major G. Denis, the pilot Capt. J. Claunch, Lt. Mack, and Sgt. Beaver for their whole-hearted and willing cooperation.

Our thanks are due the Trustees of the Sir D. J. Tata Trust who have financed this research. We are also grateful to Mr. D. R. D. Wadia for the loan of a Contax camera which was used in the experiment.

[21] J. Hamilton, W. Heitler, and H. W. Peng, Phys. Rev. 64, 78 (1943).

On the Scattering of Slow Mesons

M. S. SINHA
Cosmic Ray Research Unit, Indian Institute of Science, Bangalore, India
(Received August 25, 1945)

Photographs of mesons of total energy lying between 1.55×10^8 and 2.55×10^8 ev have been obtained by a special arrangement of counters controlling the expansion of the cloud chamber. The scattering of these particles, both multiple and single, has been studied in two thicknesses of lead (2 cm and 4 cm). It is found that though the $\sqrt{t}$ law of Williams holds good for the average angle of scattering, its absolute value is only about 50 percent of the theoretical value expected from William's formula. The Gaussian distribution of the number of particles with angle of scattering is found to be approximately true. A cross section for the non-Coulombian nuclear scattering has been calculated. The value of this is found to be 1.84×10^{-26} per nucleon for mesons of mean total energy 2×10^8 ev. This agrees satisfactorily with that calculated by Bhabha and Weinberg and Ma for transversely polarized mesons of this energy, but does not agree with that found experimentally by Shutt and Code. Our value is about twenty-five times the value obtained by Shutt. The too low value of Shutt and others may be attributed to the presence of high energy mesons (for which the nuclear scattering cross section is very small) in large numbers so as to mask the effect of low energy mesons. One case of a high energy proton being singly scattered has also been obtained.

INTRODUCTION

EXPERIMENTS on the scattering of mesotrons by plates of copper, lead, and gold have been done by Wilson[1] and also by Code,[2] the latter using a 3.5-cm tungsten plate as the scattering material. In these experiments the energy of the mesons photographed varies from 2×10^8 to about 2×10^9 ev. Both these experiments confirm the Gaussian distribution of the number of particles as a function of the product of the energy E and the scattering angle θ, and they also confirm within experimental errors the theoretical mean value of $E\theta$ as expected from Williams[3] formula. On the other hand the experiments of Fowler and Oppenheimer[4-6] *et al.* on the scattering of electrons of mean energy between 6 and 11 Mev in lead give only about 50 percent of the mean angle expected theoretically from Williams' formula. Vargus has measured the scattering angle of some 55 particles of energy below 5×10^8 ev and finds the mean value of $E\theta$ 40 percent higher than the theoretical value. He is not, however, sure whether this result is outside experimental error.

In all these experiments, however, the method of measuring the energy of the particle is by measuring the curvature of its path in a magnetic field, and the scattering angle is measured by setting a cross-wire tangentially to the track of the particle below and above the scattering plate. Wilson[1] says that the accuracy of the measurements cannot be stated with certainty. In fact there is a systematic error due to particles (positive or negative) being bent either in the same direction or in a direction opposite to the direction of scattering. The presence of a magnetic field automatically excludes some low energy particles which are curved so much as not to reach the counter below the chamber. Besides, particles scattered through large angles are helped by the magnetic field to go out of the illuminated depth of the chamber. In fact, the magnetic field always sets a lower limit to the maximum scattering angle that can be observed in the chamber.

Recently Shutt[7] has measured the scattering of a large number of particles in 1 and 5 cm of lead, where he has not used a magnetic field. He does not know the energy of the particles photographed, not even their energy distribution, very

[1] J. G. Wilson, Proc. Roy. Soc. **A174**, 73 (1940).
[2] F. L. Code, Phys. Rev. **59**, 229 (1941).
[3] E. J. Williams, Proc. Roy. Soc. **A169**, 531 (1939).
[4] W. A. Fowler and J. R. Oppenheimer, Phys. Rev. **54**, 22 (1938).
[5] N. L. Oleson, K. T. Chao, J. Halpern, and H. R. Crane, Phys. Rev. **56**, 482 (1939).
[6] C. W. Sheppard and W. A. Fowler, Phys. Rev. **57**, 273 (1939).
[7] R. P. Shutt, Phys. Rev. **61**, 6 (1942).

accurately as he uses a 16-cm lead plate above the chamber, and this shifts the energy-spectrum by a considerable amount. Shutt has not tried to confirm Williams' formula. He has assumed Williams' equation and has calculated by an ingenious method the average nuclear scattering cross section of the mesons photographed. His value seems to be too low for a meson of spin 1, but agrees fairly well with the average value of Marshak and Weisskoff[8] if we assume Hartree's energy distribution. In view of the theoretical calculations of Bhabha,[9] Weinberg,[10] and Ma[11] all of which show a maximum of the cross section for a certain energy and then a falling off on both sides, I have tried to measure the scattering of mesons of different energy intervals in the way described below. The contents of this paper are concerned only with low energy mesons.

EXPERIMENTAL

The counter arrangement that controls the expansions of the chamber is shown in Fig. 1. Counter-pairs C_1, C_2, C_3 are in coincidence and the three counters A (which are in parallel) are in anti-coincidence with $C_1C_2C_3$. We can place lead of any thickness up to 6 cm between C_3 and A and also up to 25 cm between C_2 and C_3. In the present experiment, the thickness of lead between C_3 and A is 6 cm, and there is no lead between C_2 and C_3. A 2-cm lead plate was used as the scattering material in the first part of the experiment and a plate 4 cm thick in the second part. The 9-cm lead plate placed above the top counters is used only to cut out the soft component. From the arrangement it is obvious that mesons of range more than 2 cm but less than 8 cm are photographed in the first series, and those having a range between 4 and 10 cm are photographed in the second series. The lead plate above the chamber excludes electrons and slows down some high energy mesons. From the range energy relation of mesons as given by Rossi,[12] the kinetic energies of the mesons photographed in the first series lie between 0.55×10^8 ev and 1.3×10^8 ev, and one meson of the second series lies between 0.8×10^8 ev and 1.55×10^8 ev. The energy interval in the two cases does not differ much. By placing larger amounts of lead between C_2 and C_3, we can make the energy interval shift to higher values. That is, if the thickness of lead between C_2 and C_3 is x cm, the particles photographed will have an energy corresponding to a range greater than x but less than $x+6$ cm. It is the intention to use this method to measure the scattering of mesons of higher energies also.

Before starting the experiment, the rate of counts $C_1C_2C_3$ without the anti-counters was first recorded. This gives the rate of mesotrons of all energies striking the scatterer. Next the efficiency of the anti-counters was tested in the following way. No lead was placed between the counters C_3

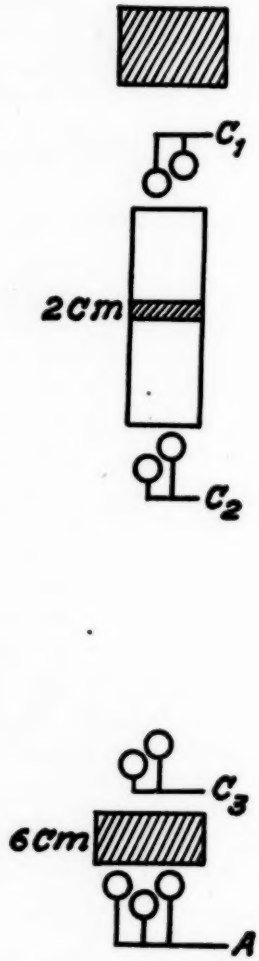

FIG. 1. Counter arrangement.

[8] R. E. Marshall and V. K. Weisskoff, Phys. Rev. **59**, 130 (1941).
[9] H. J. Bhabha, Proc. Roy. Soc. **A178**, 314 (1941); Phys. Rev. **59**, 100 (1941).
[10] J. W. Weinberg, Phys. Rev. **59**, 776 (1941).
[11] S. T. Ma and C. F. Hsuh, Proc. Camb. Phil. Soc. **40**, 171 (1944).
[12] B. Rossi and K. Greisen, Rev. Mod. Phys. **13**, 249 (1941).

TABLE I. Counting rates.

Counting arrangement	Rate of counts per hour	Thickness of lead between C_3 and A	Thickness of scatterer
$C_1C_2C_3$	28.2±0.75	0 cm	2 cm
$C_1C_2C_3-A$	0.25±0.03	0 cm	2 cm
$C_1C_2C_3-A$	1.45±0.07	6 cm	2 cm
$C_1C_2C_3-A$	1.58±0.08	6 cm	4 cm

and A and the rate of counts with the anti-counters on (i.e., $C_1C_2C_3-A$) was found to be about one in four hours which is less than one percent of the total rate. The 6-cm lead plate was now placed between C_3 and A and the rate of coincidence $C_1C_2C_3-A$ was noted for series one. This rate comes to 5.1 percent of the total rate. The rate slightly increases in the second series when the scatterer inside the chamber is 4 cm (see Table I).

It will be seen that since we do not use a magnetic field it is easier to measure the angle between the tracks of the particles above and below the scattering material, and at the same time we know that the energy of the particles lies within certain limits. The scattering angle was measured by fixing each negative between two clean glass plates on the stage of a very low power (magnification 2) microscope. This stage could be rotated. A small mirror was fixed to the periphery of this stage, and the angle of rotation of this stage was measured by a telescope and scale arrangement. As the position of the tracks in the negatives was different from different photographs, the two glass plates holding the negative between them were bodily moved until the point of intersection of the track above and below the lead plate was on the axis of the microscope. At this position the negative was rigidly fixed, and then by rotating the stage, a very fine cross-wire (which was sufficiently long to cover the whole negative) in the eyepiece was made to coincide first with the track above and then with the track below the scatterer. Half the deflection obtained in the scale divided by the distance of the scale from the mirror gave the actual angle of scattering. The accuracy with which each setting could be done was about 10′, and the mean of several settings should be accurate to 0.1°.

The defect of the above method lies principally in the fact that we do not know accurately the energy of each particle, but only know that it lies in a certain energy interval. Hence the comparison with the theory could only be made in a way slightly different from Wilson and Code.[2]

COMPARISON WITH THEORY

The theoretical development of electrical scattering of mesons and electrons is mainly owing to Williams.[3] He has taken into account screening of extra-nuclear electrons, and the arithmetic mean deflection for a finite nucleus is given by

$$J=(19.5-3.1\log_{10}z)^{\frac{1}{2}}\delta, \tag{1}$$

where

$$\delta=\frac{2(Nt)^{\frac{1}{2}}Ze^2}{Mc^2\beta^2\xi}. \tag{2}$$

$Mc^2\xi$ represents the total energy of the incident particle, for $\xi=1/(1-\beta^2)^{\frac{1}{2}}$. If E denotes the total energy, then dividing both sides of (1) by mc^2, we get upon substituting for δ

$$\frac{J}{2mc^2}=\frac{(19.5-3.1\log_{10}Z)^{\frac{1}{2}}(Nt)^{\frac{1}{2}}Ze^2}{E\beta^2\cdot mc^2}.$$

Substituting for e^2/mc^2 (classical radius of the electron) and for N (number of atoms per cc) and Z, we have

$$E\beta^2=0.906(\sqrt{t}/\theta)\times10^9 \text{ ev},$$

where θ is the average deflection in degrees.

Now the mean kinetic energy of the mesons that we have photographed is 10^8 ev, and hence the mean total energy is 2×10^8. The mean value of β^2 that we can take is, therefore, given by

$$2\cdot10^8=\mu c^2/(1-\beta^2)^{\frac{1}{2}}=10^8/(1-\beta^2)^{\frac{1}{2}},$$

or

$$\beta^2=3/4.$$

Substituting for β^2 we have finally

$$E=1.208(\sqrt{t}/\theta)\times10^9 \text{ ev}. \tag{3}$$

We shall now see how our results fit in with this theory. All the photographs were carefully analyzed, and only those tracks which have been recorded caused by the particles being stopped in the lead plate below were taken for measurement. Particles which made such large angles with the vertical that they were outside the solid angle covered by the anti-counters were excluded from measurement. Angles of scattering of individual

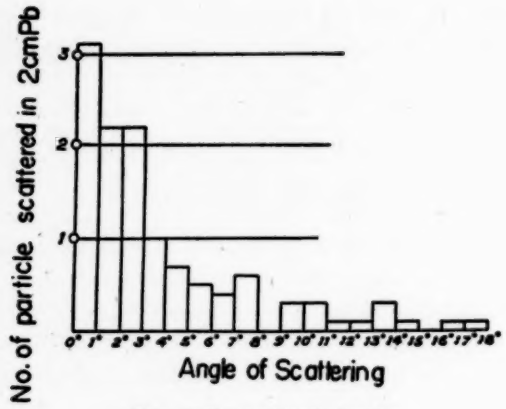

FIG. 2. Scattering in lead.

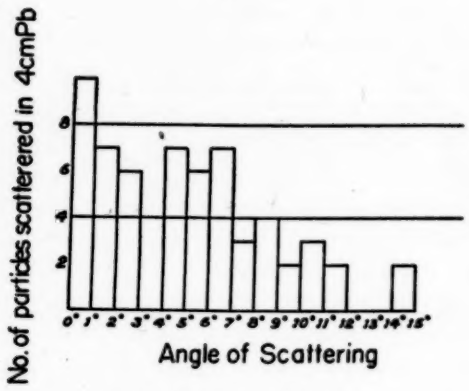

FIG. 3. Scattering in lead.

tracks being measured were classified into groups of 0° to 1°, 1° to 2°, 2° to 3°, and so on. Figure 2 shows the distribution of particles with scattering angle for $t=2$ cm, and Fig. 3 shows the same for $t=4$ cm.

The mean deflection for $t=2$ cm is $4.14°\pm.08$, for $t=4$ cm is $5.67°\pm.10$.

Equation (3) shows that if E remains constant, which is very nearly true in our case, $\theta/\sqrt{t}$ should be constant for the two thicknesses. The values of $\theta/\sqrt{t}$ for $t=2$ and 4 cm are 2.93 and 2.83, respectively. The difference in these values is about 3 percent only for an increase in $\sqrt{t}$ by a factor 1.4. Considering that for $t=4$, the value of E is a little greater than for $t=2$, we can say that the $\sqrt{t}$ law is well confirmed.

Let us now see how the mean deflection agrees with the energy. If we put $\theta=4.14°$ and $t=2$ cm in Eq. (3), we get the value of E to be 4.13×10^8 ev.

The maximum value of E possible for the 2 cm series is, however, only 2.3×10^8 ev, the minimum being 1.55×10^8 ev. If we take the energy spectrum in this interval to be smooth, the mean value of the total energy E of the particles registered is actually 1.93×10^8 ev which is only 47 percent of the value found out from William's formula. Consequently we may say that the average deflection given by Williams equations is 53 percent too large. This is not in agreement with Wilson[1] or Code,[2] who have verified Williams' equation for high energy mesons. Fowler and Oppenheimer[4-6] *et al.*, have, however, found almost the same amount of deviation for electrons of mean energy between 6 and 11 Mev, as we have found for mesons of low energy. Since the mean angle of multiple scattering for high energy mesons satisfies Williams' equation whereas the low energy mesons show a marked deviation from the theory, the cause of the discrepancy seems to depend on the energy of the mesons concerned. We have seen that the $\sqrt{t}$ law is confirmed satisfactorily, and hence the statistical effect of all the nuclei taken together agree with the theory. It therefore appears that the electrical scattering of each individual nucleus is to be modified in such a way as to give a smaller mean angle for lower energies than the theory.

NUCLEAR SCATTERING

We can see from Fig. 2 and Fig. 3 that the distribution of particles with angle of scattering shows a greater amount of deviation from Gaussian distribution for $t=4$ cm, than for $t=2$ cm. This is to be expected since the nuclear scattering cross section is proportional to the thickness of the scatterer, whereas multiple scattering varies as $\sqrt{t}$. Undoubtedly, the percentage of single scattering, which is generally large angle scattering, is more in Fig. 3 than in Fig. 2. Shutt has developed a method of calculating the average nuclear scattering cross section from the scattering data for two thicknesses of lead. The main idea is the following. If $I(\theta, t)d\theta$ represents the multiple scattering intensity between θ and $\theta+d\theta$, expressed as the percent of the total number of traversals, then instead of calculating the distribution with respect to θ we transform θ to a new variable u given by

$$u=\theta/\sqrt{t}.$$

We then have

$$f(u)=I(\theta, t)(\partial\theta/\partial u)=I(\theta, t)\sqrt{t},$$

where $f(u)du$ is the number of particles in the range between u and $u+du$. If the scattering is entirely multiple, the $f(u)$ values for all angles would be identical for the two thicknesses of lead except, however, for statistical fluctuations. Following Shutt we have calculated the $f(u)$ numbers, in the range of u from 2 to 12 for both the thicknesses, and they are given in Table II. Summing up the $f(u)$ numbers we find that instead of an equality the value for the 4 cm thickness is greater than that for 2 cm by

$$\delta=116.8-56.4=50.4.$$

The method used by Shutt for calculating the number of singly scattered particles is not strictly correct. The difference between the figures in the second and third columns of Table II shows that multiple scattering due to the electric charge of the nucleus is not the only scattering that prevails. We therefore proceed as follows. We assume that $I(\theta, t)$ represents the sum of multiply and singly scattered particles I_m and I_s, respectively, so that

$$I(\theta, t)=I_m+I_s.$$

I_s is directly proportional to the thickness of the scatterer, and consequently we can write

$$I_s=kt,$$

where k gives the percentage singly scattered in 1 cm of lead.[13] That is

$$I(\theta, t)=I_m+kt,$$

or

$$f(u)=I(\theta, t)\sqrt{t}=(I_m+Kt)\sqrt{t}=I_m(\sqrt{t})+kt^{\frac{3}{2}}.$$

Since for multiple scattering $I_m\sqrt{t}$ remains constant for different values of t, δ the difference between the values of $f(u)$ for $t=4$ and $t=2$ will be given by

$$\delta=K(4^{\frac{3}{2}}-2^{\frac{3}{2}})=5.172K.$$

The experimental value of δ is 50.4, which gives

$$K=9.73\pm2.4 \text{ percent.}$$

The statistical error has been calculated in the same way as Shutt. According to Shutt a correction of 30 percent is to be added to this for using the projections of the angles in the plain of the cloud chamber instead of the actual angles in three dimensions. Making this correction, the single scattering in one centimeter of lead comes to

$$K=12.65\pm3.2 \text{ percent.}$$

The average cross section σ per nucleon is given by

$$\sigma=K/N,$$

where N is the number of nucleons per cubic centimeter of the material, since K is the percentage scattered in 1 cm of the material. Inserting values we get

$$\sigma=\frac{12.65\times10^{-2}}{6.024\times10^{23}\times11.4}=1.84\times10^{-26}$$

±25 percent per nucleon.

This is about twenty-five times the average value obtained by Shutt for the whole energy distribution. Bhabha[9] has calculated the nuclear scattering cross section for tranversely polarized mesons taking radiation reaction into account according to the classical theory. Taking the constant $g_2^2\kappa^2/\hbar=1/13.3$, as is required by the theory of nuclear forces, he finds that the cross section attains a maximum of 3×10^{-26} for $E=3.5\mu c^2$ or 3.5×10^8 ev. The mean value of our small energy spectrum is 2×10^8 ev, and the value of the cross section found in this experiment agrees very well with Bhabha's theoretical value 1.6×10^{-26} for this energy. Recently Ma and Hsueh[11] have calculated the nuclear scattering cross section for transverse mesons according to the quantum theory, and their value is 2×10^{-26} cm^2 per nucleon for $E=2\times10^8$ ev. Weinberg's[10] theoretical value of the cross section for mesons of

TABLE II. Values of $f(u)$.

$u=\theta/\sqrt{t}$ degrees $\times$ cm$^{\frac{1}{2}}$	$I(\theta, t)\sqrt{t}=f(u)$ $t=2$ cm % $\times$ cm$^{\frac{1}{2}}$	$t=4$ cm % $\times$ cm$^{\frac{1}{2}}$
2– 4	27.1	70.8
4– 6	13.5	34.0
6– 8	6.8	6.0
8–10	5.6	3.0
10–12	3.4	3.0
2–12	56.4	116.8

[13] k is a function of θ but not of t. The K that occurs in the formula for δ further down is the integral of this k over all θ.

FIG. 4. Track of ionizing particle scattered in a 4-cm lead plate.

spin $\frac{1}{2}$ is of the same order of magnitude as ours, and agrees better with our value than with Shutt's. The experimental value of the cross section obtained by Shutt should be necessarily lower than ours since his value is an average for the whole energy spectrum. The presence of high energy mesons in large numbers completely masks the higher value of the cross section for low energy mesons. This is the reason why Wilson[1] or Code[2] (as calculated by Shutt[7]), who have deliberately excluded mesons of energy below 2×10^8 ev, get values for the nuclear scattering cross section which are too low. Here on the contrary, we have excluded the high energy mesons, and hence the value that we obtain agrees better with theoretical values for low energy mesons.

SCATTERING OF A PROTON

Figure 4 shows the track of a heavily ionizing particle being scattered through an angle of 5.6°, in a 4-cm lead plate. The track cannot be that of a meson, for if it were a meson slow enough to produce such large ionization it would not have penetrated the 4-cm plate of lead.

The range of the particle lies between 4 and 10 cm of lead and hence the minimum kinetic energy possible for the particle, taking it to be a proton is 10^8 ev, or the total energy is 10^9 ev. The mean angle of multiple scattering for this energy, according to Eq. (3) is 2.4°. The probability that a proton of this energy be scattered through 5.6° (the observed angle) is 7.3 percent. It will be still lower if the range is nearer to 10 cm. So the scattering seems to be more probably a nuclear one. There is another alternative. The charge of the particle may be more than one. If the incident particle is of charge Ze, the right-hand side of Eq. (3) is to be multiplied by Z. If we take the particle to be doubly-charged, the mean angle would come to 4.8° which is not very different from the observed angle. This alternative cannot be excluded as the ionization produced by the particle is almost that of an α-particle and this is what would be expected for a doubly-charged proton.

The author wishes to express his grateful thanks to Professor H. J. Bhabha for suggesting the experiment and his inspiring guidance throughout the work. He also wishes to thank Professor Sir C. V. Raman for lending the apparatus used for measuring the scattering angles.

Thermal Neutron Scattering Studies in Metals

FOSTER C. NIX* AND GEORGE F. CLEMENT
Bell Telephone Laboratories, New York, New York

(Received April 12, 1945)

The interaction of slow or C neutrons can be modified by changes in the physical parameters of the material which the neutrons are traversing. Measurements of the effect of grain size on *total* C neutron cross section were made on randomly-oriented poly-crystalline iron and copper. In the case of copper it was found that the total cross section decreased in an exponential manner with increase in grain size. For iron it was simply established that the total cross section was substantially smaller for the larger grain size.

THE work of Nix, Beyer, and Dunning[1] has shown that the presence of order in binary iron-nickel alloys, in which the grain size was maintained constant and free of preferred orientation, decreased the cross section below that obtained from random alloys: the greater the degree of order, the lower the total cross section obtained. The establishment of such an effect[1,2] illustrates that thermal neutrons may be used as a tool to study the structure of the solid state. In order to render this tool more useful for our systematic studies of order-disorder transformations in alloys, it was necessary to establish the influence of other physical parameters on the neutron scattering. As our first problem in this series of studies, we selected the effect of grain size. Grain growth frequently takes place in the thermal treatments necessary to produce order-disorder transformation. As metals we selected copper as a non-ferromagnetic face-centered cubic metal free from polymorphic transformations, and iron as a ferromagnetic body-centered cubic metal subject to polymorphic transformations.

EXPERIMENTAL ARRANGEMENT AND PROCEDURE

The neutron source was a radium-beryllium bulb containing 200.5 mg of radium and 8.0 mg of beryllium. Figure 1 shows the detailed arrangement of the "howitzer," scatterer, ionization chamber, amplifier, and counting circuit. Thermal neutrons from the "howitzer" passed down a cylindrical collimating tube 10 cm in diameter. The interior wall of the tube was lined with cadmium. The collimating tube contained a 0.635-cm hollow outer shell which was filled with B_4C in order to reduce the number of neutrons escaping into the room. The length of collimating tube from source to test sample was 27 cm. The collimating tube was constructed in two parts permitting samples to be placed in the neutron beam at the center of the system. The collimating tube between sample and detector was 26 cm long which prevented the C neutrons scattered at an angle of greater than 8 degrees from reaching the detector.

The neutron detector was a BF_3 ionization chamber connected to a linear amplifier and scaling system recorder located in a distant room in the laboratory building.

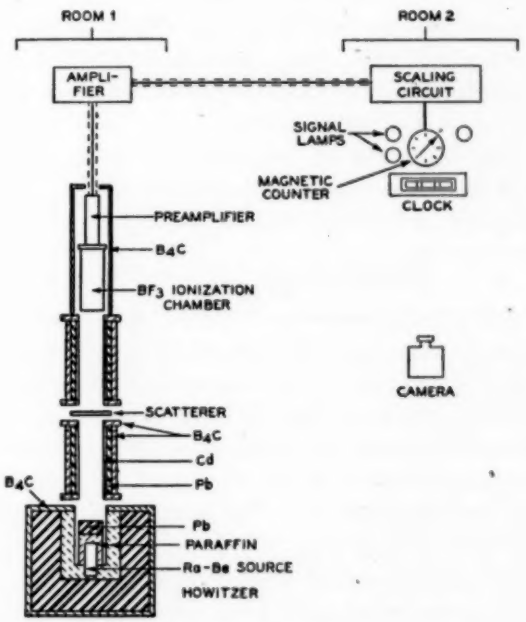

FIG. 1. Experimental arrangement.

* Now with the Research Laboratories of The Sharples Corporation, Philadelphia, Pennsylvania.

[1] F. C. Nix, H. G. Beyer, and J. R. Dunning, Phys. Rev. **58**, 1031 (1940).

[2] H. G. Beyer and M. D. Whitaker, Phys. Rev. **57**, 976 (1940).

The samples to be tested were automatically introduced into and removed from the neutron beam by electric motors. The sequence of operation of the motors was controlled by a timing circuit which provided for the following neutron beam conditions:

1. Open beam.
2. Cadmium slab in beam.
3. Sample and cadmium slab in beam.
4. Sample in beam.

When comparing the relative transmission of two samples we use the 1, 2, and 4 conditions with the cadmium replaced by the second sample. The 1 condition permitted us to keep a frequent check on amplifier and scaling circuit conditions. The timing circuit actuated the motors to operate at intervals varying from 3 to 60 minutes. All measurements in this research were carried out at 80-minute cycles, which allowed 20 minutes for each part of the cycle.

The data were recorded automatically by photographing simultaneously the counter, an electric clock which could be read to 0.1 second, and signal lamps. The use of the clock permitted the duration of each part of the cycle to be accurately measured. The combination of the three signal lamps gave positive information as to which of the above-listed beam conditions prevailed at any instant. A 16-mm motion picture camera, provided with a feature allowing the exposure of one frame at a time, was used to photograph the data, which included clock, signal lamps, and counter. Exposures were taken at intervals of 45 seconds.

The thickness of the scattering sample was such that it removed approximately 40 percent of neutrons from the "open" beam.

PREPARATION OF SAMPLES

The copper samples were prepared from an ingot of very pure deoxidized high conductivity copper by hot-working plates of the material at a temperature of 1000°C to 50 percent of their initial thickness of 3.05 cm, cold working to a thickness of 0.76 cm, and milling to a final thickness of 0.63 cm. The samples were plates $12.7\times12.7\times0.63$ cm.

The various grain sizes were obtained by annealing the cold worked material. The annealed iron sample was obtained by vacuum annealing at 1000°C for 30 minutes. Seven copper samples were prepared by vacuum annealing for 30 minutes at each of the following temperatures, 450°C, 500°C, 550°C, 650°C, 750°C, 800°C, 850°C, while an eighth sample was annealed at 1000°C for one hour. Cold worked samples of iron and copper were also retained.

The grain sizes of all scattering samples were obtained from photomicrographs of the polished and etched specimen. The qualitative orientation of the crystallites in each sample was established from x-ray diffraction patterns taken at grazing angles. The x-ray and microscopic examinations were made on the portion of the specimen exposed to the neutron beam.

METHOD OF MEASUREMENTS

a. Relative Neutron Transmission Measurements

The relative neutron transmission measurements simply consist in obtaining the transmission of two identically-shaped plates in the neutron beam. The number of counts per minute, N_a, registered in the ionization chamber with annealed sample as scatterer, is compared with the number obtained with cold worked sample as scatterer, N_b.

The transmission of the annealed sample relative to the cold worked sample, T_{ab}, is expressed by,

$$T_{ab}=\frac{N_a-N_b}{N_b}\times100. \qquad (1)$$

The final value of relative transmission was taken as the average of 36 cycles.

b. Measurement of Total Cross Section of Scatterer

The total cross section is obtained from the following four measurements:

1. The number of disintegrations produced in the BF_3 ionization chamber per minute, N_1, by the open beam with no scatterer present.
2. The number of disintegrations per minute, N_2, with 0.45 g/cm^2 of cadmium in the neutron beam.
3. The number of disintegrations per minute, N_3, with both cadmium and the scatterer whose cross section is to be determined in the beam.
4. The number of disintegrations per minute, N_4, with the scatterer alone in the neutron beam.

The cadmium in parts 2 and 3 of the cycles serves to prevent any thermal neutrons from reaching the ionization chamber.

The transmission, T, of the scatterer for C neutrons can then be determined from the following equation,

$$T=(N_4-N_3)/(N_1-N_2). \quad (2)$$

The total cross section of the scatterer can be calculated from the equation,

$$T=e^{-\sigma nt} \quad (3)$$

where σ is the total cross section in sq. cm; n, the number of nuclei per cubic cm of scatterer; and t, the thickness of the scatterer in cm. The number of nuclei per cm^3 can be obtained from the formula,

$$n=d\times 6.02\times 10^{23}/\text{Atomic weight}, \quad (4)$$

where 6.02×10^{23} is Avogadro's number and d is the density of the scatterer.

The cross-section values given in Tables I and II were taken from the average of 18 determinations. The number of neutrons recorded in the ionization chamber in the open beam condition was approximately 1000 per minute.

DISCUSSION OF RESULTS

The percent changes in transmission, referred to the cold worked sample, for measurements on iron and copper samples are given in Table I. These values are obtained from Eq. (1). They show the annealed samples to possess the larger transmission; with random orientation of crystallites, the larger the grain size the greater the transmission.

The total cross-section values, σ, obtained on cold worked and annealed samples are given in Table II. These values were obtained by the use of the Eq. (3) from transmission values obtained from Eq. (2). In Table II is also included information on preparation of samples, values of grain sizes determined microscopically, and comments on the orientation of the crystallites.

TABLE I. Relative thermal neutron cross sections.

Material	Preparation of sample	Grain size in millimeters	Orientation	Percent change in transmission referred to cold worked sample
Fe	Cold worked	0.077	Random	+7±2.0
Fe	Annealed ½ hr. 1000°C	0.127	Random	
Cu	Cold worked	0.005	Random	+9±2.0
Cu	Annealed ½ hr. 1000°C	0.081	Random	

TABLE II. Thermal neutron cross section as a function of grain size $\times 10^{24}$ cm^{-2}.

Material	Preparation of sample	Grain size in millimeters	Orientation	Total cross-section σ, $\times 10^{24}$ cm^{-2}
Fe	Cold worked	0.077	Random	13.06±0.4
Fe	Annealed ½ hr. 1000°C	0.127	Random	11.39±0.3
Cu	Cold worked	0.005	Random	10.84±0.3
Cu	Annealed ½ hr. 450°C	0.017	Random	10.16±0.4
Cu	Annealed ½ hr. 500°C	0.015	Random	10.13±0.5
Cu	Annealed ½ hr. 550°C	0.021	Random	9.96±0.4
Cu	Annealed ½ hr. 650°C	0.036	Random	9.62±0.3
Cu	Annealed ½ hr. 750°C	0.373	Random	7.76±0.2
Cu	Annealed ½ hr. 800°C	0.567	Random	7.58±0.3
Cu	Annealed ½ hr. 850°C	0.640	Random	7.37±0.4
Cu	Annealed 1 hr. 1000°C	2.40	Random	7.04±0.3

A plot of total C neutron cross section, σ, *versus* grain size for copper is given in Fig. 2. The *larger* the grain size, the smaller the *total cross section*. It is to be noted from Table II that all samples were free from any detectable preferred orientation of the crystallites. These results clearly show that the total C neutron cross sections of solid material cannot be looked upon as physical constants of the elements or compounds in question but are largely determined by the diffraction effects within the body of the scatterer. With experimental arrangement given in Fig. 1 each Bragg reflection tends to remove neutrons from the well collimated beam, causing them to be deflected to the cadmium-lined collimator tube wall and consequently removing them from the beam. For *completely randomly* oriented crystallites, the greater the number of crystallites intercepting the beam the greater the decrease in the transparency of the sample. The data in Tables I and II and the graphical illustration of the copper data in Fig. 2 clearly show the increase in transparency with the consequent decrease in total cross section

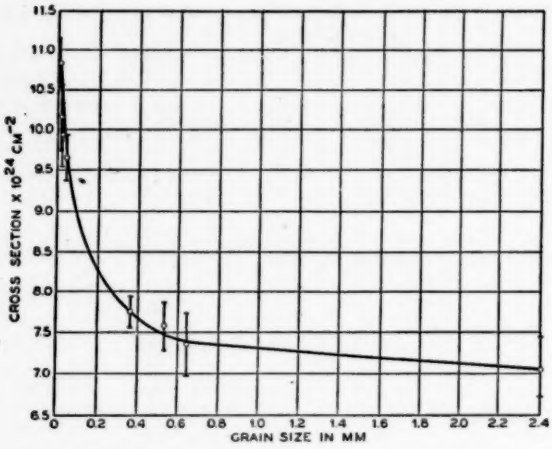

FIG. 2. Grain size *vs.* cross section $\times 10^{24}$ cm^{-2} for copper.

with increasing grain size. With random orientation, the larger the grain size, the fewer grains are available for Bragg reflection.

These experiments clearly show that the thermal neutron cross-section values given in literature lose much of their supposed quantitative significance and should be regarded as purely qualitative in nature. As an illustration, the values for copper depend to a large extent on the grain size and would be further complicated by the presence of preferred orientation. In the case of alloys there is the additional complication of atomic distribution in solid solutions and spatial distribution of phases for heterogenous binary alloys. In the work of Nix, Beyer, and Dunning[1] on iron-nickel alloys in the region around 75 atomic percent nickel, it was shown that the presence of ordering tends to increase the transparency to thermal neutrons. In this work the grain size was maintained constant while varying the degree of order, and there was demonstrated an increase of as much as 8 percent in transparency on increasing the degree of order.

As stated in the introduction, this investigation was undertaken with the object of exploring the possible use of neutrons as a tool for investigating the solid state. In order to evaluate properly data obtained at elevated temperatures on order-disorder or other solid-state transformations, it was found to be necessary to establish the effect of parameters such as grain size and change in orientation of crystallites on neutron cross-section values.

It appears that the use of thermal neutrons with wave-lengths comparable to the interatomic spacings in crystals will be a very useful method for studying the structure of the solid state. Accurate quantitative information permitting unequivocal interpretation of changes in the solid state must await the development of intense sources of monochromatic neutron beams; however, much valuable information can be obtained from the use of a relatively weak radium-beryllium source of wide wave-length bands such as were used in the present investigation.

Calculation of the Binding Energy of the Deuteron and the Neutron-Proton Scattering by a New Potential

MU-HSIEN WANG
Department of Physics, National University of Chekiang, Kweichow, Meitan, China

(Received March 6, 1945)

The binding energy of the deuteron and the scattering cross section of the proton by fast neutrons are calculated by using new forms of nuclear potential suggested by K. C. Wang. Results obtained are found to be in good agreement with experimental values when "zero cut-off" of the potential is employed.

I. INTRODUCTION

IT has been pointed out by K. C. Wang[1] that the force between two nuclear particles may be related to the gravitational force. He considers two alternative forms of the nuclear potential:

$$V=-Ae^{k/r}, \tag{1a}$$

and

$$V=-(B/r)e^{k/r}, \tag{1b}$$

with

$$k=\hbar/mc=3.84\times10^{-11}\text{ cm},$$

where the constants A and B, as determined by the gravitational constants, are 4.78×10^{-45} and 1.83×10^{-55}, respectively.

The purpose of the present work has been to determine whether the potential (1a) and (1b) can be used to obtain satisfactory values for the binding energy of the deuteron and the scattering cross section of the neutron by the proton. The calculations follow closely those of Bethe and Bacher.[2]

II. THE BINDING ENERGY OF THE DEUTERON

The wave equation for the relative motion of the two nuclear particles is

$$\Delta\psi+(M/\hbar^2)(E-V)\psi=0. \tag{2}$$

The potential is spherically symmetric. Equation (2) can thus be separated in polar co-ordinates r, θ, ϕ, by putting

$$\psi(r,\theta,\phi)=(1/r)u_lP_{lm}(\theta)e^{im\phi},$$

where P_{lm} is a spherical harmonic. The wave equation for u_l is then

$$\frac{\hbar^2}{M}\left(\frac{d^2u_l}{dr^2}-\frac{l(l+1)}{r^2}u_l\right)+(E-V)u_l=0.$$

For the ground state $l=0$, we have

$$\frac{d^2u_0}{dr^2}+\frac{M}{\hbar^2}(E-V)u_0=0. \tag{3}$$

To solve (3), two forms of potential cut-off given by (1a) and (1b) are employed;

(*a*) zero cut-off: $V=0$ for $r<a$, $V=V(r)$ for $r>a$;

(*b*) straight cut-off: $V=V(a)$ for $r<a$, $V=V(r)$ for $r>a$.

(*a*) *Zero cut-off*:—For $r<a$, $V=0$; Eq. (3) takes the form,

$$(d^2u_0/dr^2)-(M\epsilon/\hbar^2)u_0=0,$$

where $\epsilon=-E$, the binding energy of the deuteron. Its solution is

$$u_0=D\{e^{\beta r}-e^{-\beta r}\},$$

where

$$\beta=(M\epsilon/\hbar^2)^{\frac{1}{2}},$$

and

$$du_0/dr=D\beta(e^{\beta r}+e^{-\beta r}).$$

Therefore,

$$\left(\frac{1}{u_0}\frac{du_0}{dr}\right)_{r=a}=\beta\coth\beta a. \tag{4}$$

For $r>a$, $V=V(r)$; the asymptotic solution of Eq. (3) is

$$u_0=ce^{-\beta r}.$$

Treating c as a slowly varying quantity whose second derivative with respect to r may be set

[1] K. C. Wang and H. L. Tsao, Phys. Rev. **66**, 155 (1944); Nature **155**, 512 (1945).
[2] H. A. Bethe and R. E. Bacher, Rev. Mod. Phys. **8**, 82 (1936).

equal to zero, we have

$$\frac{du_0}{dr}=\frac{dc}{dr}e^{-\beta r}-\beta ce^{-\beta r},\quad \frac{d^2u_0}{dr^2}=-2\beta\frac{dc}{dr}e^{-\beta r}+\beta^2ce^{-\beta r}.$$

Substituting this last expression in (3), we get the differential equation for c,

$$\frac{dc}{dr}=-\frac{MV}{2\beta\hbar^2}c,$$

the solution of which is

$$c=F\exp\left(-\int\frac{MV}{2\beta\hbar^2}dr\right).$$

Thus

$$u_0=F\exp\left(-\beta r-\int\frac{MV}{2\beta\hbar^2}dr\right),$$

and

$$\left(\frac{1}{u_0}\frac{du_0}{dr}\right)_{r=a}=\frac{M|V(a)|}{2\beta\hbar^2}-\beta. \tag{5}$$

In order that the wave function u_0 could be joined smoothly at $r=a$ the expressions (4) and (5) must be equal; i.e.,

$$\frac{M|V(a)|}{2\beta\hbar^2}-\beta=\beta\coth\beta a. \tag{6}$$

(*b*) *Straight cut-off.*—For $r<a$, $V=V(a)$; Eq. (3) takes the form,

$$\frac{d^2u_0}{dr^2}+\frac{M}{\hbar^2}(V_0-\epsilon)u_0=0.$$

Its solution is

$$u_0=G\sin\gamma r,$$

with

$$\gamma=\left\{\frac{M}{\hbar^2}(|V(a)|-\epsilon)\right\}^{\frac{1}{2}}.$$

Thus

$$\left(\frac{1}{u_0}\frac{du_0}{dr}\right)_{r=a}=\gamma\cot\gamma a.$$

For $r>a$, $[(1/u_0)(du_0/dr)]_{r=a}$ is the same as given by (5). Therefore, instead of (6), we have

$$\frac{M|V(a)|}{2\beta\hbar^2}-\beta=\gamma\cot\gamma a. \tag{6a}$$

Equations (6) and (6a) serve to determine the binding energy of the deuteron, if we use the experimental value of $-V(a)=V_0$ (the depth of the potential well) and calculate a (the range of the nuclear force) from (1a) or (1b). Conversely, if we use the experimental value of ϵ, we can calculate the value of V_0 and a by the aid of the Eqs. (1a) or (1b).

(*c*) *Numerical calculation.*—(1) $V=0$, for $r<a$; $V=V(r)=-Ae^{k/r}$, for $r>a$. We take the recent experimental value, $V_0=10.5$ Mev, then a calculated from (1a) is equal to 4.21×10^{-13} cm. Equation (6) becomes numerically

$$\coth[1.24\times10^{15}(V_0-\epsilon)^{\frac{1}{2}}a]=(V_0/2\epsilon)-1. \tag{7}$$

From Table I we see that the root of (7), the binding energy of deuteron, is 3.60×10^{-6} erg or 2.26 Mev.

(2) $V=0$, for $r<a$; $V(r)=-(B/r)\epsilon^{k/r}$, for $r>a$. Also take $V_0=10.5$ Mev, then $a=4.42\times10^{-13}$ cm. from (1b).

From Table II we get the binding energy of the deuteron, 3.66×10^{-6} erg or 2.30 Mev. The results given by (1) and (2) are in good agreement with the experimental value 2.27 Mev.

(3) $V=V(a)$, for $r<a$; $V(r)=-Ae^{k/r}$, for $r>a$. Also take $V_0=10.5$ Mev, then $a=4.20\times10^{-13}$ cm from (1a). Equation (6a) becomes numerically

$$\cot[1.24\times10^{15}(V_0-\epsilon)^{\frac{1}{2}}a]=\frac{0.5V_0/\sqrt{\epsilon}-\sqrt{\epsilon}}{(V_0-\epsilon)^{\frac{1}{2}}}.$$

TABLE I. Values for Eq. (7).

ϵ, 10^{-6} erg	$\coth[1.24\times10^{15}(V_0-\epsilon)^{\frac{1}{2}}a]$	$V_0/2\epsilon-1$
3.50	1.33	1.38
3.60	1.32	1.32
3.70	1.31	1.26

TABLE II. Values for Eq. (7).

ϵ, 10^{-6} erg	$\coth[1.24\times10^{15}(V_0-\epsilon)^{\frac{1}{2}}a]$	$V_0/2\epsilon-1$
3.50	1.29	1.38
3.60	1.29⁻	1.32
3.70	1.27	1.26
3.80	1.27⁻	1.19

(4) $V=V(a)$, for $r<a$; $V(r)=-(B/r)e^{k/r}$, for $r>a$. We get the results listed in Table III.

From Tables III and IV, the binding energy of the deuteron is 8.0×10^{-6} and 8.3×10^{-6} erg, respectively. These values are too large in com-

TABLE III. Values for Eq. (6a).

ϵ, 10^{-6} erg	cot $[1.24\times10^{13}(V_0-\epsilon)^{\frac{1}{2}}a]$	$0.5V_0/\sqrt{\epsilon}-\sqrt{\epsilon}$ $(V_0-\epsilon)^{\frac{1}{2}}$
7.8	0.018	0.067
8.0	0.038	0.037
8.2	0.061	0.027

TABLE IV. Values for Eq. (6a).

ϵ, 10^{-6} erg	cot $[1.24\times10^{13}(V_0-\epsilon)^{\frac{1}{2}}a]$	$0.5V_0/\sqrt{\epsilon}-\sqrt{\epsilon}$ $(V_0-\epsilon)^{\frac{1}{2}}$
8.2	−0.020	0.206
8.3	−0.013	0.005
8.4	−0.004	−0.083

parison with the experimental value. The correct results will be obtained if we take $V_0=5.93$ Mev.

III. PROTON-NEUTRON SCATTERING

Let us denote by E the kinetic energy of a proton and a neutron in a coordinate system in which the center of gravity of the particles is at rest; this is equal to one-half of the kinetic energy of the incident neutron in a system at rest. The radial function u_l will satisfy the equation,

$$\frac{\hbar^2}{M}\left(\frac{d^2u_l}{dr^2}-\frac{l(l+1)}{r^2}u_l\right)+\{E-V\}u_l=0. \quad (8)$$

Asymptotically for large r, the solution of (8) is

$$u_l=c\sin(kr-\tfrac{1}{2}l\pi+\delta_l) \quad (9)$$

with

$$k^2=ME/\hbar^2.$$

Then the cross section $d\sigma$ i.e., the number of neutrons scattered per unit time through an angle between θ and $\theta+d\theta$, if there is one neutron crossing unit area per unit time in the incident beam,—is given by the well-known formula

$$d\sigma=\frac{\pi}{2k^2}\left|\sum_l(2l+1)P_l(\theta)(e^{2i\delta_l}-1)\right|^2\sin\theta d\theta. \quad (10)$$

It has been shown[3] that if $(1/k)\gg a$, a being the range of the force, all phases δ_l will be small except δ_0. Then

$$d\sigma=2\pi k^{-2}\sin^2\delta_0\sin\theta d\theta,$$

and

$$\sigma=\int d\sigma=4\pi k^{-2}\sin^2\delta_0. \quad (11)$$

For the ground state of the deuteron, we have already shown that

$$\left(\frac{1}{u_0^-}\frac{du_0^-}{dr}\right)_{r=a}=\left(\frac{MV_0}{2\beta\hbar^2}-\beta\right)\equiv\alpha. \quad (12)$$

Now,[3] in the present case E is positive, we should have[3]

$$\left(\frac{1}{u_0^+}\frac{du_0^+}{dr}\right)_{r=a}=\alpha-\frac{M(E+\epsilon)}{\hbar^2u_0^+u_0^-}\int_0^a u_0^+u_0^-dr,$$

$$=\alpha-\frac{\eta aM(E+\epsilon)}{\hbar^2}\equiv A, \quad (13)$$

where u_0^+ and u_0^- are u_0 functions for $r<a$, corresponding to the positive and negative values of E respectively; i.e.,

$$u_0^+=B\sin kr,\quad u_0^-=D\{e^{\beta r}-e^{-\beta r}\},$$

thus

$$\eta a=\frac{1}{u_0^+u_0^-}\int_0^a u_0^+u_0^-dr=\frac{\beta\coth\beta a-k\cot ka}{\beta^2+k^2}. \quad (14)$$

For large r,

$$\left(\frac{1}{u_0^+}\frac{du_0^+}{dr}\right)_{r=a}=k\cot(ka+\delta_0). \quad (15)$$

In order to join the wave function smoothly at $r=a$, the expressions given by (13) and (15) must be equal, thus

$$k\cot(ka+\delta_0)=A. \quad (16)$$

[3] Cf. reference 2, page 115.

TABLE V. Numerical results.

E_1 Mev	σ_0	σ	σ_{0B}	σ_B	σ (obs.)
2.15	0.85×10^{-24}	1.43×10^{-24}	1.2×10^{-24}	1.8×10^{-24}	$(0.5\text{–}0.8)10^{-24}$
1.05	1.03×10^{-24}	1.86×10^{-24}	1.6×10^{-24}	2.4×10^{-24}	$(1.1\text{–}1.5)10^{-24}$

Under the assumption that ka is small, we get

$$\cot \delta_0 = A/k, \tag{17}$$

and by (11),

$$\sigma = 4\pi/(k^2+A^2). \tag{18}$$

If η is small, $A \approx \alpha$, we have

$$\sigma_0 = 4\pi/(k^2+\alpha^2). \tag{19}$$

The numerical results are given in Table V, in which we take $V=-Ae^{k/r}$, and the values of α are obtained from the Table I at the point of joint. Corresponding to (18) and (19), Bethe and Bacher have derived the formulae: $\sigma_{0B}=4\pi\hbar^2/(\epsilon+E)$, $\sigma_B \doteq \frac{3}{2}\sigma_0$,[3] and the values calculated from these are given in the 4th and 5th columns of Table V for comparison.

It is seen that the present results are in better agreement with the experimental results than those given by Bethe and Bacher.

If we take $V=-(B/r)e^{k/r}$, the results do not differ appreciably from those given above.

In conclusion, the author wishes to express his thanks to Dr. K. C. Wang for suggesting this calculation and for helpful discussions.

PHYSICAL REVIEW VOLUME 68, NUMBERS 7 AND 8 OCTOBER 1 AND 15, 1945

Fourier Transforms of Retarded and Advanced Potentials

S. T. MA
National University of Peking, Kunming, China
(Received March 20, 1945)

The Fourier transforms of the retarded and advanced potentials of the electromagnetic field and of the wave fields of elementary particles are obtained with the help of the invariant functions of Jordan, Pauli, and Dirac, together with their generalizations. It is shown that the Fourier transforms of these potentials are closely related to those of the outward and inward moving waves given by Dirac for the scattering problems in quantum mechanics, and their connection is discussed. It is also shown that there exists a type of potentials which represents waves with frequencies of opposite signs propagating in opposite directions.

1. INTRODUCTION

JORDAN and Pauli[1] introduced into the quantum theory of electromagnetic field a function

$$\frac{\delta(x_0+|\mathbf{x}|)-\delta(x_0-|\mathbf{x}|)}{|\mathbf{x}|},$$

which plays a very important part in the commutation relations of the field variables. Following Dirac,[2] we shall denote it by $-\Delta$ and write

$$\Delta(\mathbf{X}) = \frac{\delta(x_0-|\mathbf{x}|)-\delta(x_0+|\mathbf{x}|)}{|\mathbf{x}|}, \tag{1}$$

where $\mathbf{X}$ denotes the four-vector $(\mathbf{x}, x_0)$. This Δ function is relativistically invariant and satisfies the wave equation of electromagnetic field in vacuum

$$\Box\Delta(\mathbf{X}) = 0, \tag{2}$$

with

$$\Box = \frac{\partial^2}{\partial x_0{}^2} - \nabla^2. \tag{3}$$

It can be expressed as a triple Fourier integral of the form

$$\Delta(\mathbf{X}) = \frac{1}{2\pi^2}\int \frac{\sin kx_0}{k} \exp(\pm i\mathbf{k}\cdot\mathbf{x}) d^3k, \tag{4}$$

where $k=|\mathbf{k}|$, or as a quadruple Fourier integral of the form[3]

$$\Delta(\mathbf{X}) = \frac{i}{4\pi^2}\int \Delta(\mathbf{K}) \exp(-ik_0x_0) \times \exp(\pm i\mathbf{k}\cdot\mathbf{x}) d^4k, \tag{5}$$

where $\mathbf{K}$ denotes the four-vector $(\mathbf{k}, k_0)$.

Some functions of the same type but more general than that of Jordan and Pauli appeared first in Dirac's[4] positron theory, which are in the

[1] Jordan and Pauli, Zeits. f. Physik **47**, 151 (1928).
[2] Dirac, Proc. Roy. Soc. **A180**, 1 (1942).
[3] Dirac, Ann. l'Inst. H. Poincaré **9**, 13 (1939).
[4] Dirac, Proc. Camb. Phil. Soc. **30**, 150 (1934).

notation of recent papers by Pauli,[5]

$$D(\mathbf{X})=\frac{1}{(2\pi)^3}\int\frac{\sin(k^2+\kappa^2x_0)^{\frac{1}{2}}}{(k^2+\kappa^2)^{\frac{1}{2}}}\times\exp(\pm i\mathbf{k}\cdot\mathbf{x})d^3k, \quad (6)$$

$$D_1(\mathbf{X})=\frac{1}{(2\pi)^3}\int\frac{\cos(k^2+\kappa^2x_0)^{\frac{1}{2}}}{(k^2+\kappa^2)^{\frac{1}{2}}}\times\exp(\pm i\mathbf{k}\cdot\mathbf{x})d^3k. \quad (7)$$

These functions are also relativistically invariant and satisfy the wave equations

$$(\Box+\kappa^2)D(\mathbf{X})=0, \quad (8)$$

$$(\Box+\kappa^2)D_1(\mathbf{X})=0. \quad (9)$$

As shown by Dirac, if we denote $|\mathbf{x}|$ by x,

$$D(\mathbf{X})=-\frac{1}{4\pi}\frac{1}{\kappa}\frac{\partial}{\partial x}F(x,x_0), \quad (10)$$

where

$$F(x,x_0)=\begin{cases}J_0[\kappa(x_0^2-x^2)^{\frac{1}{2}}] & (x_0>x)\\ 0 & (x>x_0>-x_0)\\ -J_0[\kappa(x_0^2-x^2)^{\frac{1}{2}}] & (x_0<x),\end{cases} \quad (11)$$

and

$$D_1(\mathbf{X})=\frac{1}{4\pi}\frac{1}{\kappa}\frac{\partial}{\partial x}F_1(x,x_0), \quad (12)$$

where

$$F_1(x,x_0)=\begin{cases}N_0[\kappa(x_0^2-x^2)^{\frac{1}{2}}] & (x_0>x,\ x_0<-x)\\ -iH_0^{(1)}[i\kappa(x^2-x_0^2)^{\frac{1}{2}}] & (x>x_0>-x).\end{cases} \quad (13)$$

The function $D(\mathbf{X})$ reduces to $\Delta(\mathbf{X})/4\pi$ when $\kappa=0$ and may be regarded as the analog of $\Delta/4\pi$ in field theories of elementary particles whose rest mass does not vanish. The function $D_1(\mathbf{X})$ reduces when $\kappa=0$ to

$$D_1(\mathbf{X})=\frac{1}{2\pi^2}\frac{1}{x^2-x_0^2}\text{ for }x\neq x_0. \quad (14)$$

The possibility of employing the D_1 function in quantized field theories has recently been discussed by Pauli.

It is of interest to point out that besides the positron theory and the general theory of second quantization there is a third type of mathematical problem in which these D functions can be used with advantage; namely, the Fourier resolution of retarded and advanced potentials of field theories which will be carried out in the present paper for both the electromagnetic field and the wave fields of elementary particles with the help of these D functions and their generalizations. The mathematical treatment will be developed on the lines of Dirac's[6] treatment of outward and inward moving waves in scattering problems of quantum mechanics. The connection between the Fourier transforms of the retarded and advanced potentials and those of the outward and inward moving waves will be discussed.

2. FOURIER TRANSFORMS OF RETARDED AND ADVANCED POTENTIALS OF ELECTROMAGNETIC FIELD

Let $\mathbf{A}(\mathbf{X})$ be a vector function with four components representing the scalar and vector potentials of the electromagnetic field when the charge and current densities are represented by a vector function $\mathbf{j}(\mathbf{X})$. It is known in classical electromagnetic theory that the function $\mathbf{A}$ satisfies the inhomogeneous wave equation

$$\Box\mathbf{A}(\mathbf{X})=4\pi\mathbf{j}(\mathbf{X}) \quad (15)$$

and that there are two independent solutions of (15) which have simple physical meanings, namely, the retarded potentials

$$\mathbf{A}(\mathbf{X})=\int\frac{\mathbf{j}(\mathbf{x}',x_0-|\mathbf{x}-\mathbf{x}'|)}{|\mathbf{x}-\mathbf{x}^2|}d^3x' \quad (16)$$

and the advanced potentials

$$\mathbf{A}(\mathbf{X})=\int\frac{\mathbf{j}(\mathbf{x}',x_0+|\mathbf{x}-\mathbf{x}'|)}{|\mathbf{x}-\mathbf{x}'|}d^3x'. \quad (17)$$

These retarded and advanced potentials may be expressed as four-dimensional integrals with the help of Dirac's δ functions, thus

$$\mathbf{A}(\mathbf{X})=\int\mathbf{j}(\mathbf{X}')\frac{\delta(x_0-x_0'\mp|\mathbf{x}-\mathbf{x}'|)}{|\mathbf{x}-\mathbf{x}'|}d^4x', \quad (18)$$

or

$$\mathbf{A}(\mathbf{X})=\int\mathbf{j}(\mathbf{X}')\frac{\delta(r_0\mp r)}{r}d^4x', \quad (19)$$

if we write $r_0=x_0-x_0'$, $\mathbf{r}=\mathbf{x}-\mathbf{x}'$, $r=|\mathbf{r}|$. Now the δ functions satisfy the relation

$$\frac{\delta(r_0-r)+\delta(r_0+r)}{2r}=\delta(r_0^2-r^2), \quad (20)$$

[5] W. Pauli, Phys. Rev. **58**, 716 (1940); Rev. Mod. Phys. **13**, 203 (1941).

[6] Dirac, Zeits. f. Physik **44**, 585 (1927); *Principles of Quantum Mechanics* (Clarendon Press, Oxford, 1935), second edition.

and (1) and (20) give us

$$\frac{\delta(r_0 \mp r)}{r} = \delta(r_0^2 - r^2) \pm \tfrac{1}{2}\Delta(\mathbf{R}), \tag{21}$$

where $\mathbf{R}$ denotes the four-vector $(\mathbf{r}, r_0)$. Formulae (19) may therefore be written

$$\mathbf{A}(\mathbf{X}) = \int \mathbf{j}(\mathbf{X}') \{\delta(r_0^2 - r^2) \pm \tfrac{1}{2}\Delta(\mathbf{R})\} d^4x'. \tag{22}$$

It has been shown by Dirac that, if we write

$$\Box_R = \frac{\partial^2}{\partial r_0} - \frac{\partial^2}{\partial r_1^2} - \frac{\partial^2}{\partial r_2^2} - \frac{\partial^2}{\partial r_3^2}, \qquad \Box_R \Delta(\mathbf{R}) = 0. \tag{23}$$

Using Dirac's method we can also show that

$$\Box_R \delta(r_0^2 - r^2) = 4\pi\delta_4(\mathbf{R}), \tag{24}$$

where

$$\delta_4(\mathbf{R}) = \delta(r_0)\delta(r_1)\delta(r_2)\delta(r_3).$$

From (21), (23), (24) it follows that

$$\Box_R \frac{\delta(r_0 \mp r)}{r} = 4\pi\delta_4(\mathbf{R}). \tag{25}$$

The relations (23)–(25) correspond to the fact that the retarded potentials, advanced potentials, and their mean values satisfy the same inhomogeneous wave equation, while the differences of the retarded and advanced potentials satisfy the homogeneous wave equation for the vacuum and are free of singularity everywhere.

Let the vector functions $\mathbf{A}(\mathbf{X})$ and $\mathbf{j}(\mathbf{X})$ be expressed as Fourier integrals in the form

$$\tilde{\mathbf{A}}(\mathbf{X}) = \frac{1}{(2\pi)^2} \int \tilde{\mathbf{A}}(\mathbf{K}) \exp(i(\mathbf{K}, \mathbf{X})) d^4k, \tag{26}$$

$$\tilde{\mathbf{j}}(\mathbf{X}) = \frac{1}{(2\pi)^2} \int \tilde{\mathbf{j}}(\mathbf{K}) \exp(i(\mathbf{K}, \mathbf{X})) d^4k, \tag{27}$$

where

$$(\mathbf{K}, \mathbf{X}) = k_0 x_0 - \mathbf{k}\cdot\mathbf{x}.$$

From (22), (26), and (27) we find

$$\tilde{\mathbf{A}}(\mathbf{K}) = \tilde{\mathbf{j}}(\mathbf{K}) \int \{\delta(r_0^2 - r^2) \pm \tfrac{1}{2}\Delta(\mathbf{R})\} \times \exp(-i(\mathbf{K}, \mathbf{R})) d^4r. \tag{28}$$

Thus the Fourier transforms of the potentials can be expressed in terms of those of the source densities if we know the Fourier transforms of the functions $\delta(r_0^2 - r^2)$ and $\Delta(\mathbf{R})$.

Now

$$\int \delta(r_0^2 - r^2) \exp(-i(\mathbf{K}, \mathbf{R})) d^4r = \int\int \frac{\delta(r_0 - r) + \delta(r_0 + r)}{2r} \exp(-ik_0 r_0 + i\mathbf{k}\cdot\mathbf{r}) d^3r dr_0 = \int \frac{\cos k_0 r \exp(i\mathbf{k}\cdot\mathbf{r})}{r} d^3r,$$

so that, on writing

$$\Delta_1(\mathbf{K}) = \frac{1}{2\pi^2} \int \frac{\cos k_0 r \exp(i\mathbf{k}\cdot\mathbf{r})}{r} d^3r, \tag{29}$$

we have

$$\int \delta(r_0^2 - r^2) \exp(-i(\mathbf{K}, \mathbf{R})) d^4r = 2\pi^2 \Delta_1(\mathbf{K}). \tag{30}$$

From (5) applied with $\mathbf{K}$ and $\mathbf{X}$ replaced by $\mathbf{R}$ and $\mathbf{K}$, we obtain

$$\tfrac{1}{2} \int \Delta(\mathbf{R}) \exp(-i(\mathbf{K}, \mathbf{R})^2) d^4r = -2\pi i^2 \Delta(\mathbf{K}). \tag{31}$$

Substituting from (30), (31) in (28), we obtain

$$\tilde{\mathbf{A}}(\mathbf{K}) = 2\pi^2 \tilde{\mathbf{j}}(\mathbf{K}) \{\Delta_1(\mathbf{K}) \mp i\Delta(\mathbf{K})\}, \tag{32}$$

a relation which expresses the Fourier transforms of the potentials in terms of those of the source densities with the help of the D functions. We have written here Δ, Δ_1 for the values of $4\pi D$, $4\pi D_1$, respectively, in the case of $\kappa = 0$.

3. A MODIFIED FORM OF RETARDED AND ADVANCED POTENTIALS

Substituting from (1) and (14) in (32) we obtain for the Fourier transforms of retarded and advanced potentials, the expressions

$$\bar{\mathbf{A}}(\mathbf{K})=4\pi\bar{\mathbf{j}}(\mathbf{K})\left\{\frac{1}{k^2-k_0^2}\mp\frac{\pi}{2}\frac{\delta(k_0-k)-\delta(k_0+k)}{k}\right\}, \quad (k^2\neq k_0^2). \tag{33}$$

The expressions on the right-hand side of (33) are not defined for $k_0=\pm k$, where the term $1/(k^2-k_0^2)$ tends to infinity. In order to give this term a definite meaning for $k_0=\pm k$, we can replace the function $1/(k^2-k_0^2)$ by the function $\pi\Delta_1/2$, defined by (29), at the points of singularity. When thus interpreted, (33) substituted in (26) gives our original formulae (19).

There is, however, another way of dealing with the singularities at $k_0=\pm k$. Following Dirac's works on scattering, we can take an integral whose integrand contains $1/(k^2-k_0^2)$ as a factor to be equal to its Cauchy principal value, e.g.,

$$\int\frac{\bar{\mathbf{j}}(\mathbf{K})\exp(i(\mathbf{K},\mathbf{X}))}{k^2-k_0^2}d^4k=\lim_{\epsilon\to 0}\int d^3k\left\{\int_{-\infty}^{-k-\epsilon}+\int_{-k+\epsilon}^{k-\epsilon}+\int_{k+\epsilon}^{\infty}\right\}dk_0\frac{\bar{\mathbf{j}}(\mathbf{K})\exp(i(\mathbf{K},\mathbf{X}))}{k^2-k_0^2}. \tag{34}$$

It will be interesting to see what result (33) gives when it is interpreted in this way.

The potentials given by (33) are

$$\mathbf{A}(\mathbf{X})=\frac{1}{\pi}\int\bar{\mathbf{j}}(\mathbf{K})\left\{\frac{1}{k^2-k_0^2}\mp\frac{\pi}{2}i\Delta(\mathbf{K})\right\}\exp(i(\mathbf{K},\mathbf{X}))d^4k,$$

$$=\frac{1}{(2\pi)^3}\int\int\bar{\mathbf{j}}(\mathbf{X}')\exp(-i(\mathbf{K},\mathbf{X}'))\left\{\frac{2}{k^2-k_0^2}\mp\pi i\Delta(\mathbf{K})\right\}\exp(i(\mathbf{K},\mathbf{X}))d^4k.$$

Hence, if we write

$$g(\mathbf{X},\mathbf{X}')=\frac{1}{(2\pi)^3}\int\left\{\frac{2}{k^2-k_0^2}\mp i\pi\Delta(\mathbf{K})\right\}\exp(i(\mathbf{K},\mathbf{R}))d^4k, \tag{35}$$

the retarded and advanced potentials may be written in the form

$$\mathbf{A}(\mathbf{X})=\int g(\mathbf{X},\mathbf{X}')\mathbf{j}(\mathbf{X}')d^4x'. \tag{36}$$

Equating the right-hand sides of (19) and (36), we find

$$g(\mathbf{X},\mathbf{X}')=\frac{\delta(r_0\mp r)}{r}. \tag{37}$$

Let us now find what expressions for $g(\mathbf{X},\mathbf{X}')$ are given by (35) when Cauchy's principal values are taken.

Consider first the integral

$$\int_{-\infty}^{\infty}\frac{1}{k_0^2-k^2}\exp(ik_0x_0)dk_0=\frac{1}{2k}\int_{-\infty}^{\infty}\left(\frac{1}{k_0-k}-\frac{1}{k_0+k}\right)\exp(ik_0x_0dk_0).$$

Since

$$\int_{-\infty}^{\infty}\frac{1}{k_0-k}\exp(ik_0x_0)dk_0=\pm\pi i\exp(ikx_0)\quad(x_0\gtrless 0),$$

$$\int_{-\infty}^{\infty}\frac{1}{k_0+k}\exp(ik_0x_0)dk_0=\pm\pi i\exp(-ikx_0)\quad(x_0\gtrless 0),$$

we have

$$\int_{-\infty}^{\infty}\frac{1}{k_0^2-k^2}\exp(ik_0x_0)dk_0=\mp\pi\frac{\sin kx_0}{k}\quad(x_0\gtrless 0), \tag{38}$$

so that

$$\int \frac{1}{k_0^2-k^2} \exp\,(i(\mathbf{K},\mathbf{X}))d^4k = \mp 2\pi^2\Delta(\mathbf{X}) \quad (x_0 \gtrless 0), \tag{39}$$

by (4). From (5), (35), and (39) we obtain

$$\begin{aligned} g(\mathbf{X},\mathbf{X}') &= \Delta(\mathbf{R}) \quad (r_0>0), \\ &= 0 \qquad (r_0<0), \end{aligned} \tag{40}$$

for the retarded potentials and

$$\begin{aligned} g(\mathbf{X},\mathbf{X}') &= 0 \qquad (r_0>0), \\ &= -\Delta(\mathbf{R}) \quad (r_0<0), \end{aligned} \tag{41}$$

for the advanced potentials.

On account of (1), formulae (37) and formulae (40), (41) agree except when $r_0=0$. On the plane $r_0=0$, (37) gives us $\delta(r)/r$ but (40) and (41) give us 0. Thus the two expressions for the function $g(\mathbf{X},\mathbf{X}')$ are the same everywhere except at the point $\mathbf{R}=\mathbf{X}-\mathbf{X}'=0$.

4. FOURIER TRANSFORMS OF RETARDED AND ADVANCED POTENTIALS IN THE CASE OF $\kappa \neq 0$

Let us now consider a U field satisfying the equation

$$(\Box+\kappa^2)U(\mathbf{X}) = 4\pi\rho(\mathbf{X}). \tag{42}$$

We assume, for simplicity, U and ρ to be scalar functions.

On expressing the functions $U(\mathbf{X})$ and $\rho(\mathbf{X})$ as Fourier integrals in the form

$$U(\mathbf{X}) = \frac{1}{(2\pi)^2}\int \tilde{U}(\mathbf{K}) \exp\,(i(\mathbf{K},\mathbf{X}))d^4k, \tag{43}$$

$$\rho(\mathbf{X}) = \frac{1}{(2\pi)^2}\int \tilde{\rho}(\mathbf{K}) \exp\,(i(\mathbf{K},\mathbf{X}))d^4k, \tag{44}$$

and substituting in (42), we find

$$(\kappa^2+k^2-k_0^2)\tilde{U}(\mathbf{K}) = 4\pi\tilde{\rho}(\mathbf{K}). \tag{45}$$

The result of dividing out (45) by the factor $(\kappa^2+k^2-k_0^2)$ is not unique, since when an arbitrary linear combination of the functions $\delta[k_0-(k^2+\kappa^2)^{\frac{1}{2}}]$ and $\delta[k_0+(k^2+\kappa^2)^{\frac{1}{2}}]$ is multiplied by $(\kappa^2+k^2-k_0^2)$ the product will vanish. Formulae (33) of Section 3 suggest that the Fourier transforms of the retarded and advanced U fields should be of the form

$$\tilde{U}(\mathbf{K}) = 4\pi\tilde{\rho}(\mathbf{K})\left\{\frac{1}{\kappa^2+k^2-k_0^2} \mp \frac{\pi}{2}i\frac{\delta[k_0^2(k^2+\kappa^2)^{\frac{1}{2}}]-\delta[k_0+(k^2+\kappa^2)^{\frac{1}{2}}]}{(k^2+\kappa^2)^{\frac{1}{2}}}\right\}. \tag{46}$$

By a piece of work analogous to that of Section 3 we find that (46) substituted in (43) gives, by (44),

$$U(\mathbf{X}) = \int g(\mathbf{X},\mathbf{X}')\rho(\mathbf{X}')d^4x', \tag{47}$$

with

$$g(\mathbf{X},\mathbf{X}') = \frac{1}{(2\pi)^3}\int\left\{\frac{2}{\kappa^2+k^2-k_0^2} \mp i\pi\frac{\delta[k_0-(k^2+\kappa^2)^{\frac{1}{2}}]-\delta[k_0+(k^2+\kappa^2)^{\frac{1}{2}}]}{(k^2+\kappa^2)^{\frac{1}{2}}}\right\} \exp\,(i(\mathbf{K},\mathbf{R}))d^4k, \tag{48}$$

which reduces to

$$\begin{aligned} g(\mathbf{X},\mathbf{X}') &= 4\pi D \qquad (r_0>0), \\ &= 0 \qquad (r_0<), \end{aligned} \tag{49}$$

and

$$\begin{aligned} g(\mathbf{X},\mathbf{X}') &= 0 \qquad (r_0>0), \\ &= -4\pi D \quad (r_0<0), \end{aligned} \tag{50}$$

for the retarded and advanced potentials, respectively. It can be seen with the help of (10) and (11) that the formulae (49) and (50) agree with the results obtained by Bhabha[7] for the meson field.

5. OUTWARD AND INWARD MOVING WAVES

The work of the last two sections was carried out on the same lines as Dirac's treatment of scattering. Dirac obtained a general result which may be stated as follows: When $|\mathbf{x}|$ is large,

$$\int \exp(i\mathbf{k}\cdot\mathbf{x}) f(\mathbf{k}) \left\{ \frac{1}{(k'^2+\kappa^2)^{\frac{1}{2}} - (k^2+\kappa^2)^{\frac{1}{2}}} \mp i\pi\delta[(k'^2+\kappa^2)^{\frac{1}{2}} - (k^2+\kappa^2)^{\frac{1}{2}}] \right\} d^3k$$
$$= -4\pi^2 (k'^2+\kappa^2)^{\frac{1}{2}} f\left(\pm k' \frac{\mathbf{x}}{x}\right) \frac{\exp(\pm ik'x)}{x}. \quad (51)$$

Dirac showed with the help of these formulae that by taking the combinations

$$\frac{1}{(k'^2+\kappa^2)^{\frac{1}{2}} - (k^2+\kappa^2)^{\frac{1}{2}}} \mp i\pi\delta[(k'^2+\kappa^2)^{\frac{1}{2}} - (k^2+\kappa^2)^{\frac{1}{2}}],$$

one can obtain wave functions which represent outward and inward moving particles, respectively. It was later shown by Møller[8] in the nonrelativistic approximation that Dirac's result holds not only for large distances from the source but throughout the whole space.

It will be interesting to find out the connection between our formulae for retarded and advanced potentials and Dirac's formulae for outward and inward moving waves. From (43) and (46) we have

$$U(\mathbf{X}) = \frac{1}{\pi} \int \tilde{\rho}(\mathbf{K}) \left\{ \frac{1}{\kappa^2+k^2-k_0^2} \mp \frac{\pi}{2} i \frac{\delta[k_0-(k^2+\kappa^2)^{\frac{1}{2}}] - \delta[k_0+(k^2+\kappa^2)^{\frac{1}{2}}]}{(k^2+\kappa^2)^{\frac{1}{2}}} \right\} \exp(i(\mathbf{K},\mathbf{X})) d^4k$$
$$= \frac{-1}{2\pi} \int \frac{\tilde{\rho}(\mathbf{K})}{(k^2+\kappa^2)^{\frac{1}{2}}} \left\{ \left[\frac{1}{k_0-(k^2+\kappa^2)^{\frac{1}{2}}} \pm \pi i \delta(k_0-(k^2+\kappa^2)^{\frac{1}{2}}) \right] \right.$$
$$\left. + \left[\frac{1}{-k_0-(k^2+\kappa^2)^{\frac{1}{2}}} \mp \pi i \delta[-k_0-(k^2+\kappa^2)^{\frac{1}{2}}] \right] \right\} \exp(ik_0x - i\mathbf{k}\cdot\mathbf{x}) d^4k. \quad (52)$$

The asymptotic values of the right-hand side of (52) for large distances are, according to (51) applied with $-\mathbf{x}$ in place of $\mathbf{x}$,

$$U(\mathbf{X}) = 2\pi \int_{-\infty}^{-\kappa} \tilde{\rho}\left[\mp (k_0^2-\kappa^2)^{\frac{1}{2}} \frac{\mathbf{x}}{x}, k_0 \right] \frac{\exp(i[k_0x_0 \pm (k_0^2-\kappa^2)^{\frac{1}{2}}x])}{x} dk_0$$
$$+ 2\pi \int_{\kappa}^{\infty} \tilde{\rho}\left[\pm (k_0^2-\kappa^2)^{\frac{1}{2}} \frac{\mathbf{x}}{x}, k_0 \right] \frac{\exp(i[k_0x_0 \mp (k_0^2-\kappa^2x)^{\frac{1}{2}}])}{x} d^3k_0, \quad (53)$$

showing that the retarded and advanced potentials correspond to the outward and inward moving waves, respectively, both for frequencies $k_0 > \kappa$ and for frequencies $k_0 < -\kappa$.

Besides the retarded and advanced potentials, there is another type of solutions of the inhomogeneous wave equations which have a simple mathematical form, namely, the potentials whose Fourier transforms are given, instead of by (46), by

$$\bar{U}(\mathbf{K}) = 4\pi\tilde{\rho}(\mathbf{K}) \left\{ \frac{1}{\kappa^2+k^2-k_0^2} \mp \frac{\pi}{2} i \frac{\delta[k_0-(k^2+\kappa^2)^{\frac{1}{2}}] + \delta[k_0+(k^2+\kappa^2)^{\frac{1}{2}}]}{(k^2+\kappa^2)^{\frac{1}{2}}} \right\}$$
$$= 4\pi\tilde{\rho}(\mathbf{K}) \left\{ \frac{1}{\kappa^2+k^2-k_0^2} \mp \pi i \delta(k_0^2-k^2-\kappa^2) \right\}. \quad (54)$$

Proceeding as in deriving (53) we find as the asymptotic values of the U fields whose Fourier trans-

[7] Bhabha, Proc. Roy. Soc. **A172**, 384 (1939).
[8] Møller, Zeits. f. Physik **66**, 513 (1930).

forms are given by (54):

$$U(\mathbf{X})=2\pi\left\{\int_{-\infty}^{-\kappa}+\int_{\kappa}^{\infty}\right\}dk_0\tilde{\rho}\left[\pm(k_0^2-\kappa^2)^{\frac{1}{2}}\frac{\mathbf{x}}{x},\,k_0\right]\frac{\exp\,(i[k_0x_0\mp(k_0^2-\kappa^2)^{\frac{1}{2}}x])}{x}. \tag{55}$$

Unlike the retarded and advanced potentials, this type of solutions either represents outward moving waves of positive frequencies together with inward moving waves of negative frequencies or represents inward moving waves of positive frequencies together with outward moving waves of negative frequencies, so that waves with frequencies of opposite signs travel in opposite directions. Such U fields may be written in the form of (47) with

$$g(\mathbf{X},\mathbf{X}')=\frac{1}{4\pi^3}\int\left\{\frac{1}{\kappa^2+k^2-k_0^2}\mp i\pi\delta(k_0^2-k^2-\kappa^2)\right\}\exp\,(i(\mathbf{K},\mathbf{R}))d^4k. \tag{56}$$

These expressions reduce to

$$g(X,X')=-2\pi i\{D_1(\mathbf{R})\pm iD(\mathbf{R})\}\quad(r_0\gtrless 0), \tag{57}$$

$$g(X,X')=2\pi i\{D_1(\mathbf{R})\mp iD(\mathbf{R})\}\quad(r_0\gtrless 0), \tag{58}$$

respectively, which are Hankel functions.

APPENDIX. PRINCIPAL VALUES OF IMPROPER INTEGRALS

Concerning Cauchy's principal value of an improper integral, the following theorem is frequently useful. Let $f(x)$ be a function such that the integral,

$$\int_{a-b}^{a+b}\frac{f_0(x)}{x-a}dx,$$

exists, where

$$f_0(x)=\frac{f(x)-f(2a-x)}{2},$$

and $b>0$. Then

$$P\int_{a-b}^{a+b}\frac{f(x)}{x-a}dx=\int_{a-b}^{a+b}\frac{f_0(x)}{x-a}dx. \tag{59}$$

For, if we write

$$f_e=\frac{f(x)+f(2a-x)}{2},$$

then

$$P\int_{a-b}^{a+b}\frac{f(x)}{x-a}dx=P\int_{a-b}^{a+b}\frac{f_0(x)}{x-a}dx+P\int_{a-b}^{a+b}\frac{f_e(x)}{x-a}dx=\int_{a-b}^{a+b}\frac{f_0(x)}{x-a}dx$$

$$+\lim_{\epsilon\to 0}\left\{\int_{a-b}^{a-\epsilon}\frac{f_e(x)}{x-a}dx+\int_{a+\epsilon}^{a+b}\frac{f_e(x)}{x-a}dx\right\}=\int_{a-b}^{a+b}\frac{f_0(x)}{x-a}dx.$$

As a corollary to this theorem we note that if $f(x)$ be expressible as Taylor's series in the form

$$f(x)=f(a)+(x-a)f'(a)+\tfrac{1}{2}(x-a)^2f''(a)+\cdots$$

and b is a small number, then

$$P\int_{a-b}^{a+b}\frac{f(x)}{x-a}dx=2bf'(a)+\cdots. \tag{60}$$

This corollary has been used in a recent paper by Hsüeh and the present writer.[9]

I wish to express my sincere appreciation of the friendly action of the United States Government in sending scientific microfilms to Chinese Universities in connection with the Cultural Relations Program of the Department of State which has greatly facilitated this work.

[9] Ma and Hsüeh, Proc. Camb. Phil. Soc. 40 (1944).

The Analysis of the Vibration-Rotation Band ω_3 for $C^{12}O^{16}_2$ and $C^{13}O^{16}_2$

ALVIN H. NIELSEN* AND Y. T. YAO**
Mendenhall Laboratory of Physics, The Ohio State University, Columbus, Ohio

(Received August 25, 1945)

The vibration-rotation band ω_3 for normal and isotopic CO_2 has been completely remeasured with a 7200 line-per-inch grating and the rotation lines of both bands are completely resolved. Identification of the rotation lines up to $J=90$ in the P branch and $J=56$ in the R branch for the band in normal CO_2 was made, while for the isotopic band they are identified to $J=94$ in the R branch and to $J=44$ in the P branch. The combination principle was applied to the new data and new values of the band centers and the rotational constants B_{000}, B_{001}, and α_3 have been determined. These new values are compared with those obtained from the earlier data.

I. INTRODUCTION

IN connection with the investigation of ω_2 of CD_3Cl at 2285 cm^{-1}, it was observed that the rotation lines of the isotopic CO_2 band, with which it overlaps, were completely resolved. As it was apparent that the resolution of the lines was much better than in the earlier work[1] on normal and isotopic CO_2, it was deemed worthwhile to reinvestigate the region of ω_3 for both molecules exhaustively.

The bands were observed on a prism-grating spectrometer with a two-meter-focus collimating mirror employing a 7200 line-per-inch replica grating made by R. W. Wood. Under ordinary conditions the amount of CO_2 in the atmosphere is so great that no transmission of radiant energy occurs in the most intense portions of ω_3 for normal CO_2. In order to map these regions it was found necessary to place large trays of Ascarite in the spectrometer and seal all cracks in the enclosing box with scotch tape. This device so reduced the CO_2 content of the air within the box that about 40 percent of the energy was now transmitted in the most intense regions.

The spectrometer slits were set to include a spectral interval of about 0.25 cm^{-1}, and the galvanometer deflections were read at frequency intervals of 0.07 cm^{-1}. These deflections were plotted as ordinates *versus* the angular position of the grating with respect to the central image as abscissae. The angle scale was later converted into a scale of frequencies in cm^{-1} by the usual relation $\nu\ (cm^{-1}) = K_r\ (cm^{-1}) \csc\theta$, where K_r is the instrument constant corrected to vacuum. K_r was determined from this relation by making a great many observations on the angular position of an intense green line of the mercury spectrum in the sixth order.

At least three complete sets of observations were made on the two bands in this region. The angular position of each line was determined from about 10 or 12 observations and in most cases are accurate within ± 0.07 cm^{-1}. The exceptions occur where a line of normal and isotopic CO_2 overlap. In the R branch of the normal CO_2 band, where the lines are closest together because of the convergence, lines separated by only 0.8 cm^{-1} were completely resolved. Where the overlapping occurs, lines separated by as little as 0.2 cm^{-1} were consistently, though not completely, resolved.

II. EXPERIMENTAL RESULTS

The Vibration ω_3 for Normal CO_2

In Fig. 1 is shown the graphical representation of ω_3 for $C^{12}O^{16}_2$ with galvanometer deflections plotted as ordinates and frequencies in cm^{-1} as abscissae. It may be seen that the resolution of the rotational structure is complete. The faint lines appearing as satellites and in between the main absorption peaks are real, as they have been repeated in all the measurements. Those lines not attributable to $C^{13}O^{16}_2$ may be caused by ω_3 of $C^{12}O^{16}O^{18}$, the center of which should lie in this region of the spectrum. Assignment of J values has been possible to $J=90$ in the P branch and to $J=56$ in the R branch. The J value given is

* The University of Tennessee, Knoxville, Tennessee.
** The National University of Peking, Kunming, China.

[1] P. E. Martin and E. F. Barker, Phys. Rev. **41**, 291 (1932); D. M. Cameron and H. H. Nielsen, Phys. Rev. **53**, 246 (1938); A. H. Nielsen, Phys. Rev. **53**, 983 (1938).

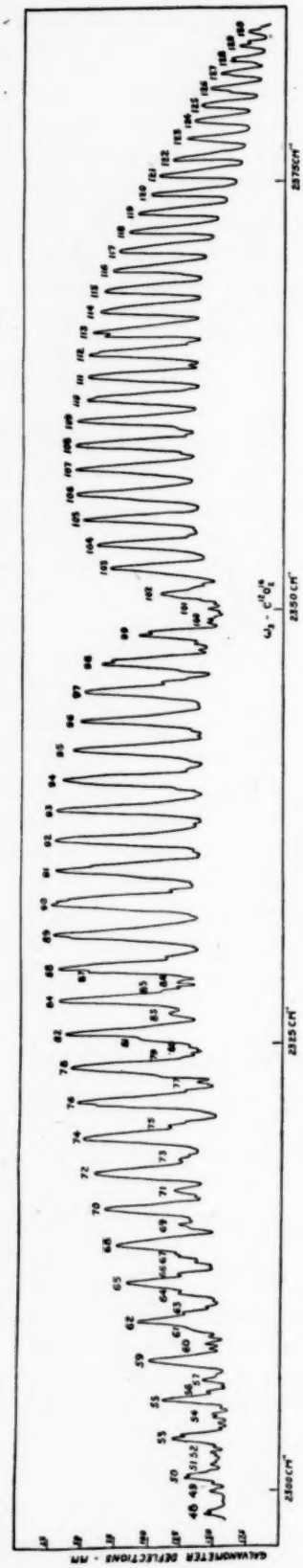

FIG. 1. Vibration-rotation band ω_3 for normal CO_2. Line numbers refer to Table I.

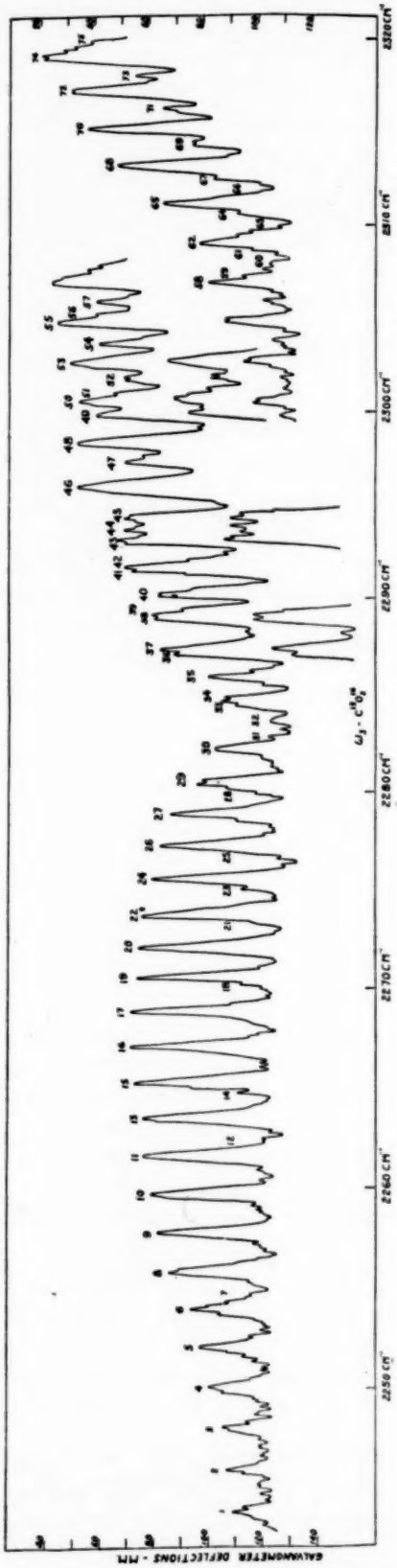

FIG. 2. Vibration-rotation band ω_3 for isotopic CO_2. Line numbers refer to Table II.

TABLE I. The rotation lines of ω_3 for $C^{13}O^{16}_2$.

Line No.	Identification	Positive branch (cm^{-1}) ν(obs.)	ν(calc.)	diff.	Line No.	Identification	Negative branch (cm^{-1}) ν(obs.)	ν(calc.)	diff.
102	$R(0)$	2350.73	2350.72	+.01					
103	$R(2)$	2352.27	2352.23	+.04	99	$P(2)$	2348.41	2348.36	+.05
104	$R(4)$	2353.77	2353.74	+.03	98	$P(4)$	2346.78	2346.76	+.02
105	$R(6)$	2355.20	2355.23	−.03	97	$P(6)$	2345.09	2345.15	−.06
106	$R(8)$	2356.75	2356.69	+.06	96	$P(8)$	2343.38	2343.50	−.12
107	$R(10)$	2358.11	2358.12	−.01	95	$P(10)$	2341.75	2341.83	−.08
108	$R(12)$	2359.59	2359.53	+.06	94	$P(12)$	2340.03	2340.13	−.10
109	$R(14)$	2360.91	2360.91	.00	93	$P(14)$	2338.37	2338.42	−.05
110	$R(16)$	2362.27	2362.27	.00	92	$P(16)$	2336.63	2336.68	−.05
111	$R(18)$	2363.61	2363.61	.00	91	$P(18)$	2334.90	2334.91	−.01
112	$R(20)$	2364.94	2364.91	+.03	90	$P(20)$	2333.06	2333.11	−.05
113	$R(22)$	2366.24	2366.20	+.04	89	$P(22)$	2331.26	2331.30	−.04
114	$R(24)$	2367.49	2367.46	+.03	88	$P(24)$	2329.40	2329.45	−.05
115	$R(26)$	2368.75	2368.70	+.05	84	$P(26)$	2327.49	2327.58	−.07
116	$R(28)$	2369.90	2369.91	−.01	82	$P(28)$	2325.70	2325.69	+.01
117	$R(30)$	2371.09	2371.09	.00	78	$P(30)$	2323.80	2323.78	+.02
118	$R(32)$	2372.24	2372.25	−.01	76	$P(32)$	2321.88	2321.84	+.04
119	$R(34)$	2373.39	2373.39	.00	74	$P(34)$	2319.88	2319.87	+.01
120	$R(36)$	2374.51	2374.51	.00	72	$P(36)$	2317.93	2317.87	+.06
121	$R(38)$	2375.62	2375.58	+.04	70	$P(38)$	2315.86	2315.86	.00
122	$R(40)$	2376.55	2376.65	−.10	68	$P(40)$	2313.85	2313.82	+.03
123	$R(42)$	2377.73	2377.69	+.04	65	$P(42)$	2311.77	2311.75	+.02
124	$R(44)$	2378.71	2378.70	+.01	62	$P(44)$	2309.68	2309.66	+.02
125	$R(46)$	2379.71	2379.68	+.03	59	$P(46)$	2307.54	2307.55	−.01
126	$R(48)$	2380.60	2380.65	−.05	56	$P(48)$	2305.41	2305.41	.00
127	$R(50)$	2381.57	2381.59	−.02	53	$P(50)$	2303.26	2303.24	+.02
128	$R(52)$	2382.47	2382.50	−.03	50	$P(52)$	2301.06	2301.05	+.01
129	$R(54)$	2383.32	2383.38	−.06	48	$P(54)$	2298.93	2298.83	+.10
130	$R(56)$	2384.21	2384.25	−.04	46	$P(56)$	2296.57	2296.59	−.02
					44	$P(58)$	2294.29	2294.33	−.04
					41	$P(60)$	2292.02	2292.04	−.02
					38	$P(62)$	2289.75	2289.73	+.02
					36	$P(64)$	2287.48	2287.39	+.09
					34	$P(66)$	2285.12	2285.03	+.09
					31	$P(68)$	2282.55	2282.64	−.09
					28	$P(70)$	2280.31	2280.22	+.09
					25	$P(72)$	2277.79	2277.79	.00
					23	$P(74)$	2275.29	2275.32	−.03
					21	$P(76)$	2272.84	2272.83	+.01
					18	$P(78)$	2270.56*	2270.32	+.24
						$P(80)$	*	2267.79	
					14	$P(82)$	2265.10	2265.21	−.11
					12	$P(84)$	2262.62	2262.64	−.02
						$P(86)$	*	2260.02	
						$P(88)$	*	2258.39	
					7	$P(90)$	2254.68	2254.73	−.05

that for the ground state.[2] In the region where the P branch of normal CO_2 and the R branch of the isotopic molecule overlap, the positions are somewhat less accurately known, and identification is therefore a little more difficult and uncertain. In Table I are listed the observed frequencies, corrected to vacuum, of the lines in ω_3 of normal CO_2 with the assigned J values. Each line in Fig. 1 is numbered and can be identified by referring to Table I. In adjacent columns of Table I are found the line frequencies computed with the use of constants determined from the data. It may be seen that the mean difference is less than 0.01 cm^{-1}. The lines in Table I marked with an asterisk are either unobserved or somewhat in error because of overlapping with the isotopic band.

[2] The nuclear spin of the oxygen atoms is zero, and for this reason the part of the wave function depending on the nuclear spin is always symmetrical to an interchange of the two identical oxygen atoms. As a result of the exclusion principle, which requires that the total wave function shall belong to a certain class, only the levels characterized by even J values are present in the normal state. The effect is that every other line in the spectrum is absent, i.e., only $R(J)$ and $P(J)$ with even values of J will occur.

The Vibration ω_3 for Isotopic CO_2

Figure 2 shows the graphs of the galvanometer deflections *versus* the frequencies in cm^{-1} for ω_3

TABLE II. The rotation lines of ω_3 for $C^{13}O^{16}_2$.

Line No.	Identification	Positive branch (cm^{-1}) ν(obs.)	ν(calc.)	diff.	Line No.	Identification	Negative branch (cm^{-1}) ν(obs.)	ν(calc.)	diff.
33	$R(0)$	2284.91	2284.92	−.01					
35	$R(2)$	2286.44	2286.44	.00	30	$P(2)$	2282.67	2282.56	+.11
37	$R(4)$	2287.84*	2287.95	−.11	29	$P(4)$	2280.95	2280.98	−.03
39	$R(6)$	2289.51	2289.43	+.08	27	$P(6)$	2279.35	2279.38	−.03
40	$R(8)$	2290.81	2290.88	−.07	26	$P(8)$	2277.72	2277.70	+.02
42	$R(10)$	2292.31	2292.31	.00	24	$P(10)$	2275.99	2276.04	−.05
43	$R(12)$	2293.72	2293.72	.00	22	$P(12)$	2274.23	2274.34	−.11
45	$R(14)$	2294.99	2295.09	−.10	20	$P(14)$	2272.62	2272.62	.00
46	$R(16)$	2296.57	2296.45	+.12	19	$P(16)$	2270.70*	2270.47	+.23
47	$R(18)$	2297.88	2297.77	+.11	17	$P(18)$	2269.24	2269.10	+.14
48	$R(20)$	2299.02	2299.07	−.05	16	$P(20)$	2267.30	2267.30	.00
49	$R(22)$	2300.35	2300.25	+.10	15	$P(22)$	2265.52	2265.47	+.05
51	$R(24)$	2301.43*	2301.60	−.17	13	$P(24)$	2263.67	2263.62	+.05
52	$R(26)$	2302.35*	2302.82	−.47	11	$P(26)$	2261.78	2261.75	+.03
54	$R(28)$	2304.15*	2304.02	+.13	10	$P(28)$	2259.69	2259.85	−.16
55	$R(30)$	2305.19	2305.18	+.01	9	$P(30)$	2257.98	2257.91	+.07
57	$R(32)$	2306.40	2306.36	+.04	8	$P(32)$	2256.00	2255.95	+.05
58	$R(34)$	2307.45	2307.46	−.01	6	$P(34)$	2253.93	2253.98	−.05
60	$R(36)$	2308.54	2308.55	−.01	5	$P(36)$	2252.05	2251.97	+.08
61	$R(38)$	2309.42*	2309.63	−.11	4	$P(38)$	2249.97	2249.95	+.02
63	$R(40)$	2310.62	2310.67	−.05	3	$P(40)$	2247.96	2247.89	+.07
64	$R(42)$	2311.51*	2311.67	−.16	2	$P(42)$	2245.93	2245.82	+.11
66	$R(44)$	2312.58*	2312.69	−.11	1	$P(44)$	2243.83	2243.70	+.13
67	$R(46)$	2313.52*	2313.65	−.13					
	$R(48)$	*	2314.86						
69	$R(50)$	2315.08	2315.05	+.03					
	$R(52)$	*	2315.96						
71	$R(54)$	2316.89	2316.83	+.06					
	$R(56)$	*	2318.07						
73	$R(58)$	2318.90	2318.90	.00					
	$R(60)$	*	2319.70						
75	$R(62)$	2320.50	2320.47	+.03					
	$R(64)$	*	2321.19						
	$R(66)$	*	2321.91						
	$R(68)$	*	2322.60						
77	$R(70)$	2322.90	2322.93	−.03					
	$R(72)$	*	2323.89						
79	$R(74)$	2324.34*	2324.21	+.13					
80	$R(76)$	2324.80*	2324.99	−.19					
81	$R(78)$	2325.51*	2325.65	−.14					
	$R(80)$	*	2326.17						
83	$R(82)$	2326.77	2326.79	−.02					
	$R(84)$	*	2327.17						
	$R(86)$	*	2327.64						
85	$R(88)$	2328.22	2328.15	+.07					
86	$R(90)$	2328.51	2328.46	+.06					
	$R(92)$	*	2328.83						
89	$R(94)$	2329.18	2329.19	−.01					

of the isotopic molecule. Several lines have been redrawn from other data in Fig. 2 to show how well small details were reproduced from one set of observations to another. Because of the overlapping of the two bands, the lines are not as completely resolved nor quite as accurately known in the R branch of this band as in the P branch or as in ω_3 of the normal molecule. Assignment of J values to lines has, however, been possible to $R(94)$ and to $P(44)$ with a few exceptions where the overlapping precluded the observation of the individual lines. The observed frequencies are listed in Table II with the appropriate J value for the lower state.[2] The lines in Fig. 2 are numbered and can be identified by referring to Table II. The line frequencies computed from constants determined from the data, are found in adjacent columns in Table II. Because of overlapping with the normal molecule band, a number of lines are either in error or unobserved and are marked with an asterisk. The average difference between the observed and computed frequencies is about 0.02 cm^{-1}.

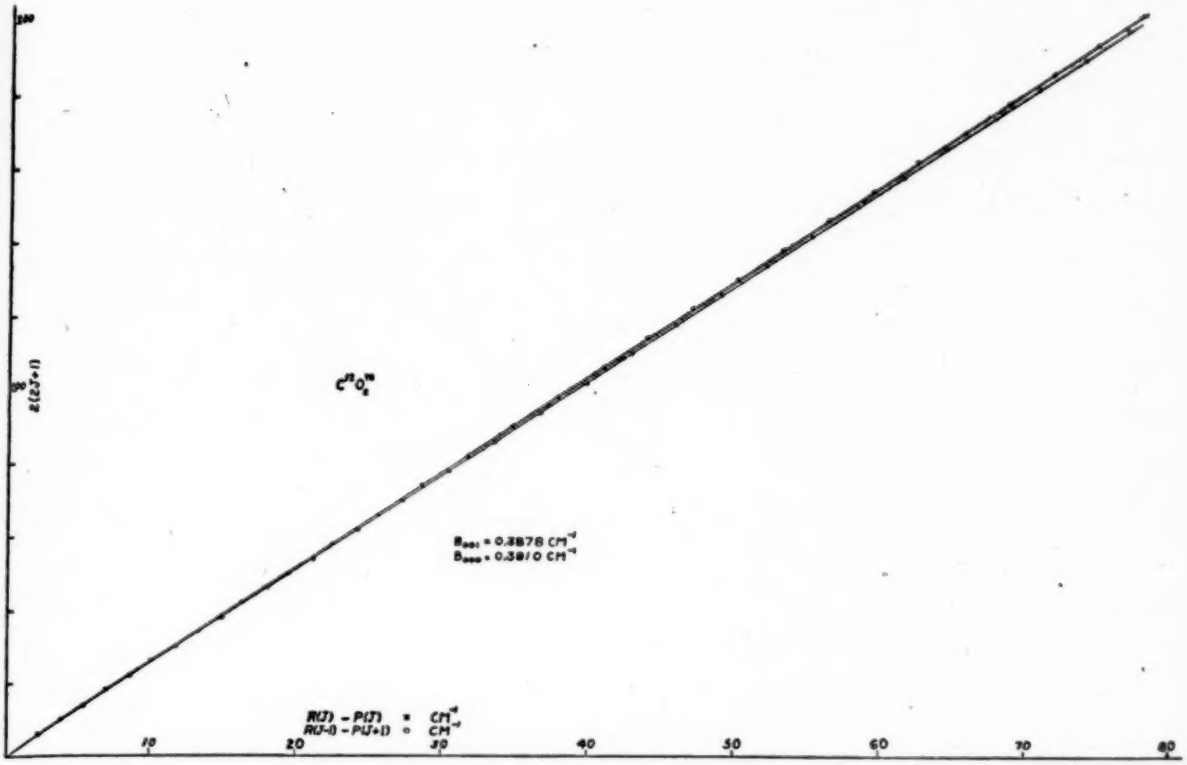

FIG. 3. Plots of $R(J-1)-P(J+1)$ and $R(J)-P(J)$ *versus* $2(2J+1)$ for ω_3 of normal CO_2.

III. DISCUSSION OF THE RESULTS

The combination principle[3] has been applied to the bands measured, with the result that an accurate direct determination of the constants relating to the vibration ω_3 were possible. The energy expressions for the rotational levels in the normal and first excited vibrational states are, respectively:

$$E''/hc = E_{000}/hc + J''(J''+1)B_{000} - J''^2(J''+1)^2D,$$

and (1)

$$E'/hc = E_{001}/hc + J'(J'+1)B_{001} - J'^2(J'+1)^2D.$$

B_{000} and B_{001} are constants ($B=h/8\pi^2Ic$) representing the moments of inertia in the ground and first vibration states, and D is the centrifugal stretching constant. It may be shown for this molecule that, to a good approximation, D may be neglected. The rotation lines on the high frequency side of the band center form the R branch and are given by:

$$R(J)=\omega_0+(J+1)(B_{001}+B_{000}) + (J+1)^2(B_{001}-B_{000}),$$

while the lines on the low frequency side form the P branch and are given by

$$P(J)=\omega_0-J(B_{001}+B_{000})+J^2(B_{001}-B_{000}),$$

where J is the quantum number of total angular momentum in the lowest state, and ω_0 is the band center or the frequency of the $J=0$ line. By combining these relations properly, the following expressions, from which B_{000} and B_{001} emerge, may be obtained:

$$R(J-1)-P(J+1)=2(2J+1)B_{000}$$

and (2)

$$R(J)-P(J)=2(2J+1)B_{001}.$$

Figures 3 and 4 show graphs of these two equations with term differences in cm^{-1} plotted as abscissae and $2(2J+1)$ as ordinates for both molecules. The slopes of these lines yield B_{000} and B_{001}, respectively. B_e, the equilibrium value of B,

[3] G. Herzberg, *Infrared and Raman Spectra of Polyatomic Molecules* (Van Nostrand, New York, 1945), p. 390.

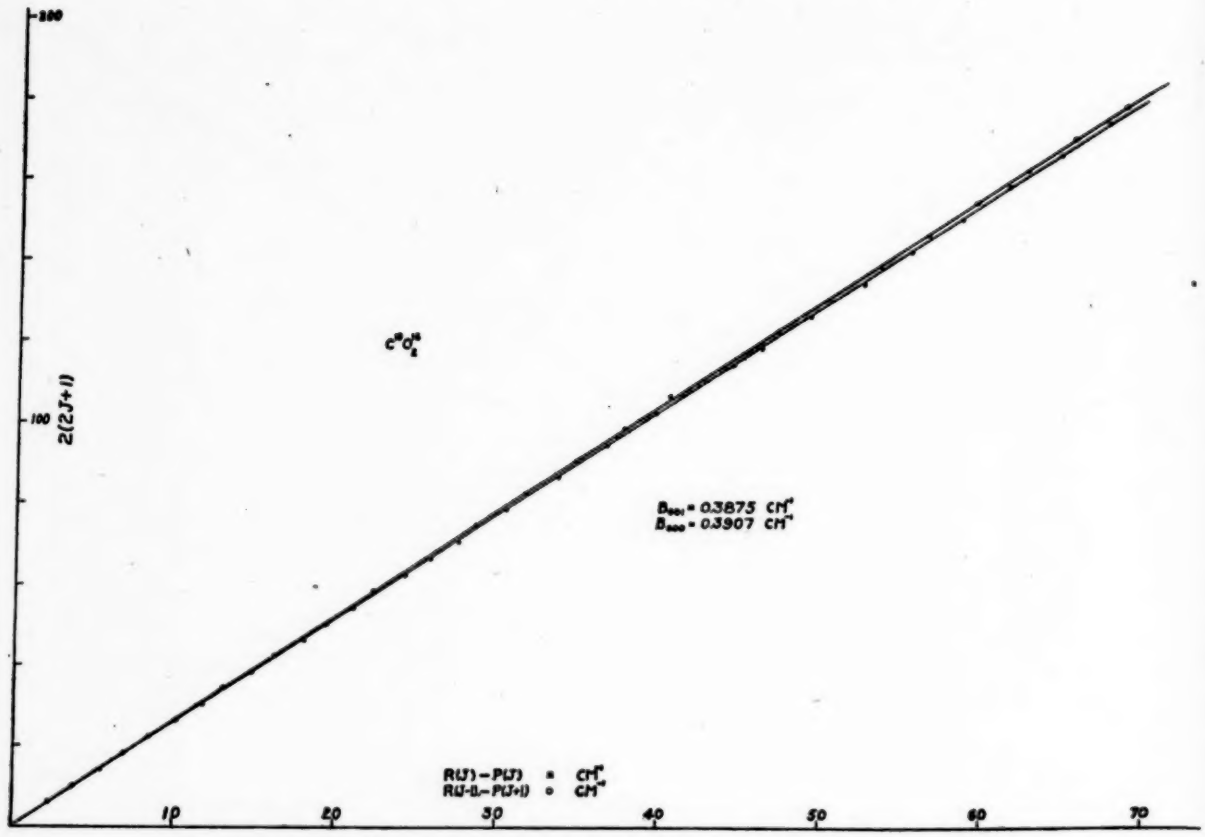

FIG. 4. Plots of $R(J-1)-P(J+1)$ and $R(J)-P(J)$ *versus* $2(2J+1)$ for isotopic CO_2.

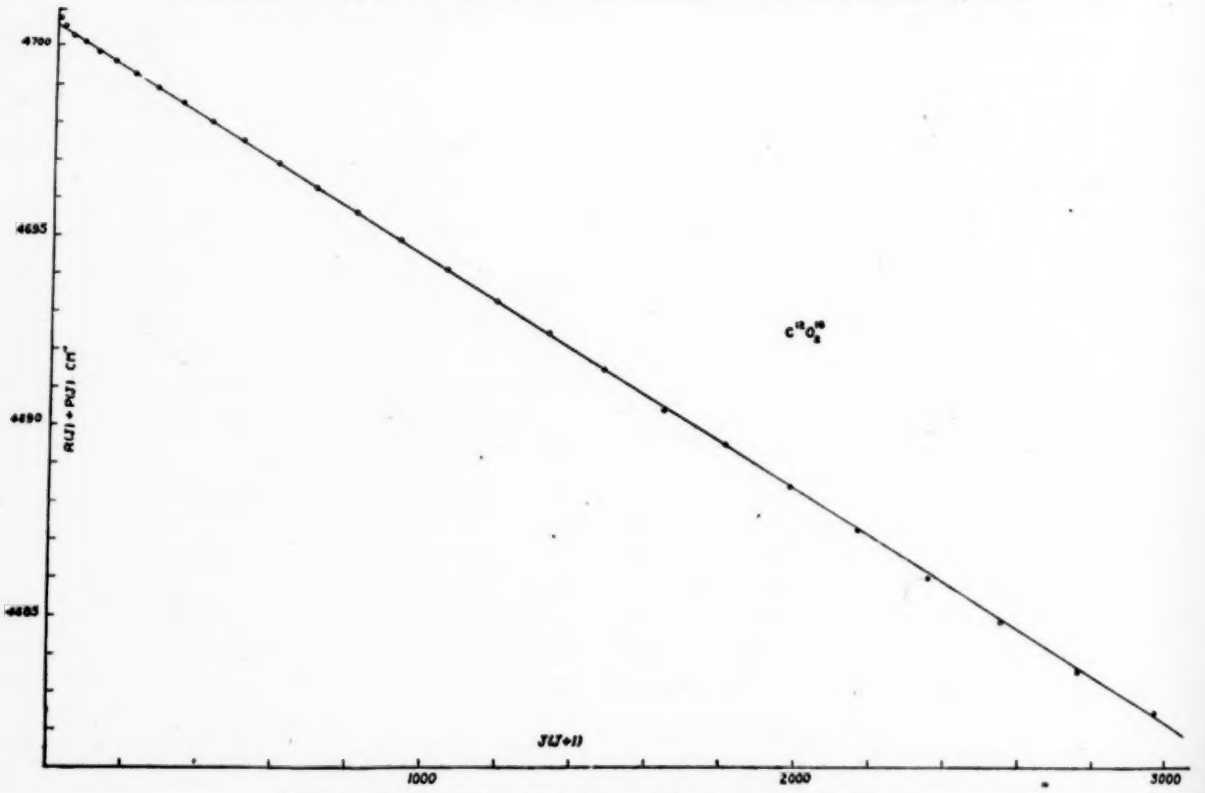

FIG. 5. Plot of $R(J)+P(J)$ *versus* $J(J+1)$ for normal CO_2.

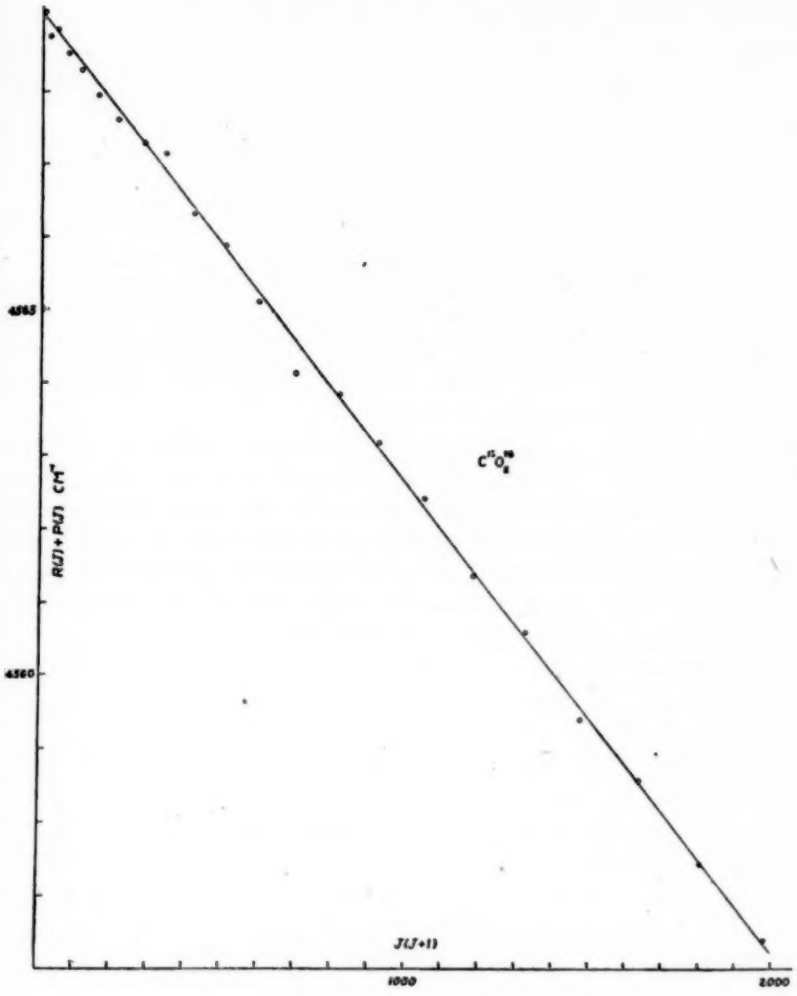

FIG. 6. Plot of $R(J)+P(J)$ *versus* $J(J+1)$ for isotopic CO_2.

and the equilibrium internuclear distances may be obtained from B_{000} and B_{001} and the convergence factors α_1, α_2, α_3 with the relation:

$$B_v=B_e-\alpha_1(v_1+\tfrac{1}{2})-\alpha_2(v_2+1)-\alpha_3(v_3+\tfrac{1}{2}). \quad (3)$$

The frequency, ω_0, of the $J=0$ line may be obtained from another combination relation, namely:

$$R(J)+P(J)=2(\omega_0+B_{001}) +2J(J+1)(B_{001}-B_{000}). \quad (4)$$

When $R(J)+P(J)$ in cm^{-1} is plotted *versus* $J(J+1)$, as in Figs. 5 and 6, a straight line results, the intercept of which is $2(\omega_0+B_{001})$ and the slope of which is $2(B_{001}-B_{000})$ or $-2\alpha_3$. The values of the various constants obtained from the present data follow in Table III.

IV. CONCLUSION

The B_{000} and B_{001} found in columns 1 and 2 of Table III are obtained directly as the slopes of the curves in Figs. 3 and 4, and the differences between these values give α_3 or $B_{000}-B_{001}$ in column 3. Another value of α_3, found in column 4, is obtained directly from the slopes of the curves given in Figs. 5 and 6. From a theoretical relation for α_3 given by Nielsen[4] and utilizing values of the vibrational frequencies of ω_1, ω_2, ω_3, the potential energy constant c given by Dennison,[5] and a value of B_e, the computed value of α_3, found in column 5, was obtained. It may be seen that these determinations of α_3 are in excellent

[4] A. H. Nielsen, J. Chem. Phys. 11, 160 (1943).
[5] D. M. Dennison, Rev. Mod. Phys. 12, 175 (1940).

TABLE III. Values of the constants relating to ω_3 for $C^{12}O^{16}_2$ and $C^{13}O^{16}_2$.

	B_{000} (cm^{-1})	B_{001} (cm^{-1})	α_3 (cm^{-1}) i.e., ($B_{000}-B_{001}$) from Col. 1–Col. 2	α_3 (cm^{-1}) from Figs. 5 and 6	α_3 (cm^{-1}) calc. from reference (4)	ω_3 (cm^{-1}) band center
$C^{12}O^{16}_2$	0.3910	0.3878	0.0032	0.0031	0.0031	2349.93
$C^{13}O^{16}_2$	0.3907	0.3875	0.0032	0.0032		2284.14

agreement with each other, but do not agree with $\alpha_3=0.0029$ cm^{-1} given by Herzberg.[6] The combination principle applied to Martin and Barker's[1] data on ω_2 yields a value for B_{000} of 0.3903. This is in reasonably good agreement with the value in Table III. The value $B_{000}=0.3895$ cm^{-1} given by Herzberg[6] appears to be low. When the combination principle is applied to Barker and Adel's data[7] on $\nu_3-(\nu_1, 2\nu_2)$ it yields values for B_{001} of $B_{001}=0.3861$ cm^{-1} (10.41μ band) and $B_{001}=0.3862$ cm^{-1} (9.40μ band), respectively. The values of B_{001} from Barker and Adel's data, although in agreement with each other, are not consistent with the B_{001} listed in Table III, found from the present data on ω_3.

It may also be seen from Table III that the constants B_{000}, B_{001}, and α_3 for normal CO_2 are very nearly equal to the values of these constants for the isotopic molecule. This is rather good evidence that the equilibrium moment of inertia and internuclear distance and the force constants are the same for the two molecules.

[6] G. Herzberg, reference 3, p. 394–395.
[7] E. F. Barker and A. Adel, Phys. Rev. **44**, 185 (1933).

PHYSICAL REVIEW VOLUME 68, NUMBERS 7 AND 8 OCTOBER 1 AND 15, 1945

The Vibration-Rotation Energies of Polyatomic Molecules

Part II. Accidental Degeneracies

HARALD H. NIELSEN
Mendenhall Laboratory of Physics, Ohio State University, Columbus, Ohio

(Received August 22, 1945)

The first- and second-order corrections to the vibration-rotation energies of polyatomic molecules are dealt with in instances where two or more vibration frequencies are accidentally degenerate. The method of the contact transformation employed in Part I is extended and made applicable to the two types of first-order resonance interactions, i.e., the Fermi-Dennison type and the Coriolis type. The components of the energy matrix are evaluated in general, and examples are considered to demonstrate how the actual energies may be evaluated.

I. INTRODUCTION

THE vibration and rotation of a general polyatomic molecule have been dealt with quantum mechanically in an earlier paper, hereafter referred to as Part I,[1] and expressions were derived for the energies by a second-order perturbation calculation. The results are applicable, except in certain anomalous cases, to specific molecular models to obtain the vibration-rotation energies.

The perturbation method applied to this problem is related to the fact that, except for the terms of Coriolis interaction between degenerate vibrations and the rotation of the molecule, the terms in the first-order Hamiltonian, H_1, cannot in general contribute to the energy before in second order of approximation. It is, therefore, effective to transform the Hamiltonian, H_1, of the molecule by a contact transformation into $T\,H\,T^{-1}=H_0'+\epsilon H_1'+\epsilon^2 H_2'\cdots$ where H_1' will contain to second order of approximation only the above mentioned Coriolis interaction terms. Linear combinations of the zero-order wave functions may always be found so that the matrix of H_1' will have only diagonal elements. Using the stabilized wave functions of H_0', i.e., the linear combination of the zero-order wave functions which will diagonalize $H_0'+\epsilon H_1'$, the calculation of the second-order energies is reduced, in effect, to a first-order perturbation calculation.

Denoting by $T(\epsilon)$ the transformation function $e^{i\epsilon S}$, we have to second order of approximation:

$$T=1+i\epsilon S-(\epsilon^2/2)S^2+\cdots. \tag{1}$$

Transformation of $H=H_0+\epsilon H_1+\epsilon^2 H_2\cdots$ leads to $THT^{-1}=H'=H_0'+\epsilon H_1'+\epsilon^2 H_2'$ where it is readily shown that

$$H_0'=H_0,\quad H_1'=H_1-i(H_0S-SH_0),\quad H_2'=H_2+(i/2)[S(H_1+H_1')-(H_1+H_1')S]. \tag{2}$$

The method is very effective except in such cases where peculiar relationships exist between the vibration frequencies. For example, if the first-order Hamiltonian of a molecule has a term $k_{ss's''}q_{ss}q_{s's'}q_{s''s''}$ in it, the transformed second Hamiltonian, H_2', will contain a contribution inversely proportional to

$$[(\lambda_s^{\frac{1}{2}}+\lambda_{s'}^{\frac{1}{2}}+\lambda_{s''}^{\frac{1}{2}})(\lambda_s^{\frac{1}{2}}+\lambda_{s'}^{\frac{1}{2}}-\lambda_{s''}^{\frac{1}{2}})(\lambda_s^{\frac{1}{2}}-\lambda_{s'}^{\frac{1}{2}}+\lambda_{s''}^{\frac{1}{2}})(\lambda_s^{\frac{1}{2}}-\lambda_{s'}^{\frac{1}{2}}-\lambda_{s''}^{\frac{1}{2}})],$$

where $\lambda_s=4\pi^2c^2\omega_s^2$, and the anharmonic coefficients x_{ss}, $x_{ss'}$ etc., in the expression for the vibration energy of the molecule will contain terms with the same denominator (see for example, Eq. (30), Part I). If accidentally $\lambda_{s''}^{\frac{1}{2}}$ should be very nearly equal to $\lambda_s^{\frac{1}{2}}+\lambda_{s'}^{\frac{1}{2}}$ (i.e., $\omega_{s''}\approx\omega_s+\omega_{s'}$) in which case resonance is said to occur, the quantities x_{ss} and $x_{ss'}$ may become indefinitely large and the method described above will fail. A similar instance may arise when the first-order Hamiltonian, H_1, of a polyatomic molecule contains a Coriolis interaction term

$$\zeta_{ss'}[(\lambda_s/\lambda_{s'})^{\frac{1}{2}}q_{s'}p_s-(\lambda_{s'}/\lambda_s)^{\frac{1}{2}}q_sp_{s'}]P_\alpha.$$

[1] H. H. Nielsen, Phys. Rev. **60**, 794 (1941).

The transformed second-order Hamiltonian, H_2', will contain terms corresponding to those with the denominator $\lambda_s-\lambda_{s'}$. These in turn give rise to correction terms to the effective reciprocals of inertia with the same denominator. As before, if λ_s should accidentally be very nearly equal to $\lambda_{s'}$ so that resonance sets in, the correction terms may become indefinitely large, and the method described before becomes inadequate. We shall hereafter consider how the above method may be modified to take account satisfactorily of the contribution to the energies by such terms when resonance between frequencies takes place.

II. ANHARMONIC RESONANCE INTERACTIONS

We shall first consider the case where the resonance interaction results because of the presence of terms in the anharmonic portion of the potential energy which are cubic in the coordinates. The general anharmonic potential energy term which is cubic in the coordinates may be written[2]

$$hck_{ss's''}q_{ss}q_{s's'}q_{s''s''}. \tag{3}$$

This term may be removed from the first-order Hamiltonian by transforming H with the transformation function[3]

$$\begin{aligned}S=-hck_{ss's''}\{&\lambda_s^{\frac{1}{2}}(\lambda_s-\lambda_{s'}-\lambda_{s''})p_{ss}q_{s's'}q_{s''s''}/\hbar+\lambda_{s'}^{\frac{1}{2}}(\lambda_{s'}-\lambda_{s''}-\lambda_s)q_{ss}p_{s's'}q_{s''s''}/\hbar\\&+\lambda_{s''}^{\frac{1}{2}}(\lambda_{s''}-\lambda_s-\lambda_{s'})q_{ss}q_{s's'}p_{s''s''}/\hbar-2\lambda_s^{\frac{1}{2}}\lambda_{s'}^{\frac{1}{2}}\lambda_{s''}^{\frac{1}{2}}p_{ss}p_{s's'}p_{s''s''}/\hbar^3\}\\&\times\{\hbar(\lambda_s^{\frac{1}{2}}+\lambda_{s'}^{\frac{1}{2}}+\lambda_{s''}^{\frac{1}{2}})(\lambda_s^{\frac{1}{2}}+\lambda_{s'}^{\frac{1}{2}}-\lambda_{s''}^{\frac{1}{2}})(\lambda_s^{\frac{1}{2}}-\lambda_{s'}^{\frac{1}{2}}+\lambda_{s''}^{\frac{1}{2}})(\lambda_s^{\frac{1}{2}}-\lambda_{s'}^{\frac{1}{2}}-\lambda_{s''}^{\frac{1}{2}})\}^{-1}.\end{aligned} \tag{4}$$

The transformation produces, however, a term in the second-order Hamiltonian with the denominator $(\lambda_s^{\frac{1}{2}}+\lambda_{s'}^{\frac{1}{2}}-\lambda_{s''}^{\frac{1}{2}})$. When, for example, the combination frequency $\lambda_s^{\frac{1}{2}}+\lambda_{s'}^{\frac{1}{2}}$ (or overtone frequency when $s=s'$) and the fundamental $\lambda_{s''}^{\frac{1}{2}}$ are very nearly alike, resonance sets in and the term $hck_{ss's''}q_{ss}q_{s's'}q_{s''s''}$ may evidently contribute to the energy of the molecule an amount which is of first-order magnitude. It therefore appears that it is not legitimate to remove the term $hck_{ss's''}q_{ss}q_{s's'}q_{s''s''}$ from the first-order Hamiltonian. A closer inspection reveals, however, that it is only the $(v_{ss}, v_{s's'}, v_{s''s''}|v_{ss}\pm1, v_{s's'}\pm1, v_{s''s''}\mp1)$ matrix elements of this potential energy which offers difficulties. It therefore becomes apparent that if a transformation function S can be found such that after the transformation of H has taken place H_1' will contain only the elements $(v_{ss}, v_{s's'}, v_{s''s''}|v_{ss}\pm1, v_{s's'}\pm1, v_{s''s''}\mp1)$, these having, of course, the same values as the corresponding elements of the term $hck_{ss's''}q_{ss}q_{s's'}q_{s''s''}$, then a transformation method may still be employed with advantage. It will be seen that the term,

$$(hck_{ss's''}/4)\{(q_{ss}p_{s's'}+q_{s's'}p_{ss})p_{s''s''}/\hbar^2-(p_{ss}p_{s's'}/\hbar^2-q_{ss}q_{s's'})q_{s''s''}\}, \tag{5}$$

has the same $(v_{ss}, v_{s's'}, v_{s''s''}|v_{ss}\pm1, v_{s's'}\pm1, v_{s''s''}\mp1)$ matrix elements as (3), but that all its other matrix elements are equal to zero. Since the function (4) will remove the term (3) entirely from H_1', we may expect to obtain a transformation function appropriate for us by adding (4) to a function s which will put the expression (5) back into the transformed H_1'. A little experimentation shows that the function

$$\begin{aligned}s=(hck_{ss's''}/4)&\{\lambda_s^{\frac{1}{2}}+\lambda_{s'}^{\frac{1}{2}}-\lambda_{s''}^{\frac{1}{2}}+\lambda_{s''}^{\frac{1}{2}}\lambda_s-\lambda_s^{\frac{1}{2}}\lambda_{s''}-\lambda_s\lambda_{s'}^{\frac{1}{2}}-\lambda_{s'}\lambda_s^{\frac{1}{2}}-\lambda_{s'}^{\frac{1}{2}}\lambda_{s''}+\lambda_{s''}^{\frac{1}{2}}\lambda_{s'}-2\lambda_s^{\frac{1}{2}}\lambda_{s'}^{\frac{1}{2}}\lambda_{s''}^{\frac{1}{2}}\}\\&\times\{(p_{ss}p_{s's'}p_{s''s''}/\hbar^3)-(q_{ss}q_{s's'}p_{s''s''}/\hbar)+(q_{ss}p_{s's'}q_{s''s''}/\hbar)+(p_{ss}q_{s's'}q_{s''s''}/\hbar)\}\\&\times\{\hbar(\lambda_s^{\frac{1}{2}}+\lambda_{s'}^{\frac{1}{2}}+\lambda_{s''}^{\frac{1}{2}})(\lambda_s^{\frac{1}{2}}+\lambda_{s'}^{\frac{1}{2}}-\lambda_{s''}^{\frac{1}{2}})(\lambda_s^{\frac{1}{2}}-\lambda_{s'}^{\frac{1}{2}}+\lambda_{s''}^{\frac{1}{2}})(\lambda_s^{\frac{1}{2}}-\lambda_{s'}^{\frac{1}{2}}-\lambda_{s''}^{\frac{1}{2}})\}^{-1}\end{aligned} \tag{6}$$

will accomplish this. The transformation function S^* suitable for our problem will be $S^*=S+s$ and

---

[2] The coordinates q_{ss} used here are dimensionless so that if $k_{ss's''}$ is expressed in cm^{-1}, the term $hck_{ss's''}$ will have the dimensions of energy. The constants $k_{ss's''}$ used here will be found to be equivalent to the $k_{ss's''}$ used in Part I, multiplied by the constant $(\hbar^{\frac{1}{2}}/8\pi^2c^{5/2}\omega_s^{\frac{1}{2}}\omega_{s'}^{\frac{1}{2}}\omega_{s''}^{\frac{1}{2}})$.

[3] W. H. Shaffer, H. H. Nielsen, and L. H. Thomas, Phys. Rev. **56**, 895 (1939). S. Silver and W. H. Shaffer, J. Chem. Phys. **9**, 599 (1941).

is equal to

$$S^*=(hck_{ss's''}/4)\{(\lambda_s+\lambda_{s'}+\lambda_{s''}-2\lambda_s^{\frac{1}{2}}\lambda_{s'}^{\frac{1}{2}}+2\lambda_s^{\frac{1}{2}}\lambda_{s''}^{\frac{1}{2}}+2\lambda_{s'}^{\frac{1}{2}}\lambda_{s''}^{\frac{1}{2}})(p_{ss}p_{s'\sigma'}p_{s''\sigma''}/\hbar^4)-(\lambda_s+\lambda_{s'}-3\lambda_{s''}$$
$$-2\lambda_s^{\frac{1}{2}}\lambda_{s'}^{\frac{1}{2}}-2\lambda_s^{\frac{1}{2}}\lambda_{s''}^{\frac{1}{2}}-2\lambda_{s'}^{\frac{1}{2}}\lambda_{s''}^{\frac{1}{2}})(q_{ss}q_{s'\sigma'}p_{s''\sigma''}/\hbar^2)+(\lambda_s-3\lambda_{s'}+\lambda_{s''}+2\lambda_s^{\frac{1}{2}}\lambda_{s'}^{\frac{1}{2}}+2\lambda_s^{\frac{1}{2}}\lambda_{s''}^{\frac{1}{2}}$$
$$-2\lambda_{s'}^{\frac{1}{2}}\lambda_{s''}^{\frac{1}{2}})(q_{ss}p_{s'\sigma'}q_{s''\sigma''}/\hbar^2)+(-3\lambda_s+\lambda_{s'}+\lambda_{s''}+2\lambda_s^{\frac{1}{2}}\lambda_{s'}^{\frac{1}{2}}-2\lambda_s^{\frac{1}{2}}\lambda_{s''}^{\frac{1}{2}}+2\lambda_{s'}^{\frac{1}{2}}\lambda_{s''}^{\frac{1}{2}})$$
$$\times(p_{ss}q_{s'\sigma'}q_{s''\sigma''}/\hbar^2)\}\{(\lambda_s^{\frac{1}{2}}+\lambda_{s'}^{\frac{1}{2}}+\lambda_{s''}^{\frac{1}{2}})(\lambda_s^{\frac{1}{2}}-\lambda_{s'}^{\frac{1}{2}}+\lambda_{s''}^{\frac{1}{2}})(\lambda_s^{\frac{1}{2}}-\lambda_{s'}^{\frac{1}{2}}-\lambda_{s''}^{\frac{1}{2}})\}^{-1}. \quad (7)$$

It should be noted that S^* does not contain the denominator $(\lambda_s^{\frac{1}{2}}+\lambda_{s'}^{\frac{1}{2}}-\lambda_{s''}^{\frac{1}{2}})$.

We have, then, for the zero-order Hamiltonian

$$H_0=(1/2)\{(P_x^2/I_{xx}^{(e)})+(P_y^2/I_{yy}^{(e)})+(P_z^2/I_{zz}^{(e)})\}+(\hbar/2)\sum_s\sum_\sigma\{\lambda_s^{\frac{1}{2}}(p_{s\sigma}^2/\hbar^2+q_{s\sigma}^2)\}, \quad (8)$$

and for the transformed first-order Hamiltonian, H_1', the following:

$$H_1'=(hck_{ss's''}/4)\{(q_{ss}p_{s'\sigma'}+p_{ss}q_{s'\sigma'})p_{s''\sigma''}/\hbar^2-(p_{ss}p_{s'\sigma'}/\hbar^2-q_{ss}q_{s'\sigma'})q_{s''\sigma''}\}. \quad (9)$$

The transformed second-order Hamiltonian will also differ from the relation given in Eq. (21c), Part I,[4] but only insofar as the terms containing $k_{ss's''}^2$ as a coefficient are concerned. We restate, therefore, only this term. It is:

$$(i/2)(S^*H_1-H_1S^*)=(hck_{ss's''}/2)^2\{i(\lambda_s+\lambda_{s'}+\lambda_{s''}-2\lambda_s^{\frac{1}{2}}\lambda_{s'}^{\frac{1}{2}}+2\lambda_s^{\frac{1}{2}}\lambda_{s''}^{\frac{1}{2}}+2\lambda_{s'}^{\frac{1}{2}}\lambda_{s''}^{\frac{1}{2}})$$
$$\times(p_{ss}q_{ss}p_{s'\sigma'}q_{s'\sigma'}p_{s''\sigma''}q_{s''\sigma''}-q_{ss}p_{ss}q_{s'\sigma'}p_{s'\sigma'}q_{s''\sigma''}p_{s''\sigma''})/\hbar^4$$
$$-(\lambda_s+\lambda_{s'}-3\lambda_{s''}-2\lambda_s^{\frac{1}{2}}\lambda_{s'}^{\frac{1}{2}}-2\lambda_s^{\frac{1}{2}}\lambda_{s''}^{\frac{1}{2}}-2\lambda_{s'}^{\frac{1}{2}}\lambda_{s''}^{\frac{1}{2}})(q_{ss}^2q_{s'\sigma'}^2/\hbar)$$
$$+(\lambda_s-3\lambda_{s'}+\lambda_{s''}+2\lambda_s^{\frac{1}{2}}\lambda_{s'}^{\frac{1}{2}}+2\lambda_s^{\frac{1}{2}}\lambda_{s''}^{\frac{1}{2}}-2\lambda_{s'}^{\frac{1}{2}}\lambda_{s''}^{\frac{1}{2}})(q_{ss}^2q_{s''\sigma''}^2/\hbar)$$
$$+(-3\lambda_s+\lambda_{s'}+\lambda_{s''}+2\lambda_s^{\frac{1}{2}}\lambda_{s'}^{\frac{1}{2}}-2\lambda_s^{\frac{1}{2}}\lambda_{s''}^{\frac{1}{2}}+2\lambda_{s'}^{\frac{1}{2}}\lambda_{s''}^{\frac{1}{2}})(q_{s'\sigma'}^2q_{s''\sigma''}^2/\hbar)\}$$
$$\times\{2(\lambda_s^{\frac{1}{2}}+\lambda_{s'}^{\frac{1}{2}}+\lambda_{s''}^{\frac{1}{2}})(\lambda_s^{\frac{1}{2}}-\lambda_{s'}^{\frac{1}{2}}+\lambda_{s''}^{\frac{1}{2}})(\lambda_s^{\frac{1}{2}}-\lambda_{s'}^{\frac{1}{2}}-\lambda_{s''}^{\frac{1}{2}})\}^{-1}. \quad (10)$$

To arrive at the energies we proceed now by assuming that $\lambda_s^{\frac{1}{2}}+\lambda_{s'}^{\frac{1}{2}}\approx\lambda_{s''}^{\frac{1}{2}}$ so that we may write $\lambda_{s''}^{\frac{1}{2}}=\lambda_{s'}^{\frac{1}{2}}+\lambda_s^{\frac{1}{2}}+\delta$ where δ is small. When we substitute this into the portion of H_0 which concerns these frequencies we obtain

$$H_0=(\hbar/2)\{\lambda_s^{\frac{1}{2}}(p_{s\sigma}^2/\hbar^2+q_{s\sigma}^2)+\lambda_{s'}^{\frac{1}{2}}(p_{s'\sigma'}^2/\hbar^2+q_{s'\sigma'}^2)+(\lambda_s^{\frac{1}{2}}+\lambda_{s'}^{\frac{1}{2}})(p_{s''\sigma''}^2/\hbar^2+q_{s''\sigma''}^2)\}, \quad (11)$$

and

$$H_1'=(\delta\hbar/2)(p_{s''\sigma''}^2/\hbar^2+q_{s''\sigma''}^2)+(hck_{ss's''}/4)\{(q_{ss}p_{s'\sigma'}+p_{ss}q_{s'\sigma'})p_{s''\sigma''}/\hbar^2$$
$$-(p_{ss}p_{s'\sigma'}/\hbar^2-q_{ss}q_{s'\sigma'})q_{s''\sigma''}\}. \quad (12)$$

If now the frequencies are non-degenerate so that we may set $\sigma=\sigma'=1$, we obtain at once that

$$(E_0/hc)=\omega_s(v_s+v_{s''}+1)+\omega_{s'}(v_{s'}+v_{s''}+1). \quad (13)$$

The first term in H_1' has only elements diagonal in the quantum numbers and the second, as we have seen, has only the matrix elements $(v_s, v_{s'}, v_{s''}|v_s\pm1, v_{s'}\pm1, v_{s''}\mp1)$. These elements are the following

$$(v_s, v_{s'}, v_{s''}|H_1'/hc|v_s, v_{s'}, v_{s''})=(v_{s''}+\tfrac{1}{2})\Delta, \quad \Delta=(\delta/4\pi c), \quad (14a)$$

$$(v_s, v_{s'}, v_{s''}|H_1'/hc|v_s+1, v_s+1, v_{s''}-1)=(v_s+1, v_{s'}+1, v_{s''}-1|H_1'/hc|v_s, v_{s'}, v_{s''})$$
$$=k_{ss's''}[((v_s+1)/2)((v_{s'}+1)/2)(v_{s''}/2)]^{\frac{1}{2}}. \quad (14b)$$

The matrix components of the transformed second-order Hamiltonian which are of importance are those diagonal in the quantum numbers. In our case they are the same as those given in Part I

[4] To arrive at the modified expression for H_2', it is necessary to recompute the expression $(i/2)\{S^*(H_1'+H_1)-(H_1'+H_1)S^*\}$. It is quickly seen that S^* has no matrix elements of the type $(v_s'v_{s'}v_{s''}|v_s\pm1, v_{s'}\pm1, v_{s''}\mp1)$ while H_1' was so determined that it contains only elements of this type. In evaluating the energies to second-order of approximation, we shall be interested only in the elements of H_2' diagonal in the quantum numbers v_s, $v_{s'}$, $v_{s''}$, but it is evident that $(S^*H_1'-H_1'S^*)$ will have none such. It is necessary, therefore, only to consider $(S^*H_1-H_1S^*)$.

except insofar as the terms having the coefficient $k^2_{ss's''}$ are concerned. These occur in only $x_{ss'}$. In our case the term multiplied by $k^2_{ss's''}$ will be

$$-(hc/2)(k_{ss's''}/2)^2\left\{\frac{1}{\omega_s+\omega_{s'}+\omega_{s''}}+\frac{1}{\omega_s-\omega_{s'}+\omega_{s''}}-\frac{1}{\omega_s-\omega_{s'}-\omega_{s''}}\right\}. \tag{15}$$

The expression (15) will be seen to be identical to the relation occurring in $x_{ss'}$ as defined in Part I except that the term having the denominator $(\omega_s+\omega_{s'}-\omega_{s''})$ is absent.[5]

When the frequency $\lambda_s^{\frac{1}{2}}$ is equal to the frequency $\lambda_{s'}^{\frac{1}{2}}$, we have the interesting case which is generally referred to as Fermi-Dennison[6] resonance. When the frequencies $\lambda_s^{\frac{1}{2}}$ and $\lambda_{s''}^{\frac{1}{2}}$ are non-degenerate so that $\sigma=\sigma''=1$, the term in the first-order Hamiltonian which allows the resonance interaction to occur, may be written $hck_{sss''}q_s^2q_{s''}$. The appropriate transformation of this term may be achieved by using the function (7) where $s=s'$, $\sigma=\sigma'$, and where the order in which the operators occur is preserved. In this case we set $\lambda_{s''}^{\frac{1}{2}}=2\lambda_s^{\frac{1}{2}}+\delta$, δ being small, and we have for the zero-order Hamiltonian which relates to $\lambda_s^{\frac{1}{2}}$ and $\lambda_{s''}^{\frac{1}{2}}$

$$H_0=(\hbar\lambda_s^{\frac{1}{2}}/2)\{(p_s^2/\hbar^2+q_s^2)+2(p_{s''}^2/\hbar^2+q_{s''}^2)\}, \tag{16}$$

and for the transformed first-order Hamiltonian

$$H_1'=(\delta\hbar/2)(p_{s''}^2/\hbar^2+q_{s''}^2)+(hck_{sss''}/4)[(p_sq_s+q_sp_s)p_{s''}/\hbar^2-(p_s^2/\hbar^2-q_s^2)q_{s''}^2]. \tag{17}$$

For the zero-order energies we obtain at once

$$(E_0/hc)=\omega_s(v_s+2v_{s''}+\tfrac{3}{2}). \tag{18}$$

As before the first term in H_1' has only elements diagonal in the quantum numbers, while the second has the elements $(v_s, v_{s''}|v_s\pm2, v_s\mp1)$ only. These are

$$(v_s, v_{s''}|H_1'/hc|v_s, v_{s''})=\Delta(v_{s''}+\tfrac{1}{2}), \quad (\Delta=\delta/4\pi c), \tag{19a}$$

$$(v_s, v_{s''}|H_1'/hc|v_s+2, v_{s''}-1)=(v_s+2, v_{s''}-1|H_1'/hc|v_s, v_{s''})$$
$$=(k_{sss''}/2)[(v_s+1)(v_s+2)(v_{s''}/2)]^{\frac{1}{2}}. \tag{19b}$$

The diagonal elements of H_2' are again the only ones which are of interest. Their contributions to the energy can be shown to be identically the same as those give in Part I except insofar as the contributions which have the coefficient $k^2_{sss''}$ are concerned. Such terms occur only in x_{ss} and $x_{ss''}$. As in the earlier example one may show that the contributions which have the coefficient $k^2_{sss''}$ remain the same as those given in Part I except that the term which has the denominator $(2\omega_s-\omega_{s'})$ will be absent.

When the frequency $\lambda_s^{\frac{1}{2}}$ is twofold degenerate, as may be the case in linear and axially symmetric polyatomic molecules, the index σ may take the values $\sigma=1$ and $\sigma=2$. In such cases resonance may occur between the overtone $2\omega_s$ and the fundamental frequency $\omega_{s''}$ if the first-order potential energy contains the following component

$$hck_{sss''}(q_{s,1}^2+q_{s,2}^2)q_{s''}. \tag{20}$$

Here it is only the elements $(v_{s,1}; v_{s,2}; v_{s''}|v_{s,1}\pm2; v_{s,2}; v_{s''}\mp1)$ and $(v_{s,1}; v_{s,2}; v_{s''}|v_{s,1}; v_{s,2}\pm2, v_{s''}\mp1)$ which cause trouble when resonance between $2\omega_s$ and $\omega_{s''}$ occurs. The terms in (20) are properly transformed by use of (7) exactly as in the preceding example. As before we proceed by setting

---

[5] The component of $x_{ss'}$ which has $k_{ss's''}$ as a coefficient is stated in Part I as follows: $\omega_{s''}(\omega_{s''}^2-\omega_s^2-\omega_{s'}^2)/[(\omega_s+\omega_{s'}+\omega_{s''})\times(\omega_s+\omega_{s'}-\omega_{s''})(\omega_s-\omega_{s'}+\omega_{s''})(\omega_s-\omega_{s'}-\omega_{s''})]$. This may be factored into $(1/4)\left[\frac{1}{\omega_s+\omega_{s'}+\omega_{s''}}-\frac{1}{\omega_s+\omega_{s'}-\omega_{s''}}+\frac{1}{\omega_s-\omega_{s'}+\omega_{s''}}-\frac{1}{\omega_s-\omega_{s'}-\omega_{s''}}\right]$.

[6] E. Fermi, Zeits. f. Physik **71**, 250 (1931). D. M. Dennison, Phys. Rev. **41**, 304 (1932).

$\lambda_{s''}^{\frac{1}{2}}=2\lambda_s^{\frac{1}{2}}+\delta$ and obtain for the zero-order Hamiltonian the following:

$$H_0=(\hbar\lambda_s^{\frac{1}{2}}/2)\{(p_{s,1}^2/\hbar^2+p_{s,2}^2/\hbar^2+q_{s,1}^2+q_{s,2}^2)+2(p_{s''}^2/\hbar^2+q_{s''}^2)\}, \tag{21}$$

and the transformed first-order Hamiltonian will be:

$$H_1'=(\delta\hbar/2)(p_{s''}^2/\hbar^2+q_{s''}^2)+(hck_{sss''}/4)[(p_{s,1}q_{s,1}+q_{s,1}p_{s,1}+p_{s,2}q_{s,2}+q_{s,2}p_{s,2})p_{s''}/\hbar^2-(p_{s,1}^2/\hbar^2+p_{s,2}^2/\hbar^2-q_{s,1}^2-q_{s,2}^2)q_{s''}]. \tag{22}$$

It is convenient to replace the coordinates $q_{s,1}$ and $q_{s,2}$ and the conjugate momenta $p_{s,1}$ and $p_{s,2}$ by their equivalents in cylindrical coordinates. These are $q_{s,1}=r_s\cos\chi_s$, $q_{s,2}=r_s\sin\chi_s$, $p_{s,1}=(-i\hbar)[\cos\chi_s\partial/\partial r_s-(\sin\chi_s/r_s)\partial/\partial\chi_s]$ and $p_{s,2}=(-i\hbar)[\sin\chi_s\partial/\partial r_s+(\cos\chi_s/r_s)\partial/\partial\chi_s]$. The eigenvalues of (21) are known to be:

$$(E_0/hc)=(v_s+2v_{s''}+2)\omega_s. \tag{23}$$

The matrix components of H_1' rewritten in the same coordinates are known to be the following:[7]

$$(v_s, l_s, v_{s''}|H_1'/hc|v_s, l_s, v_{s''})=\Delta(v_{s''}+\tfrac{1}{2}), \quad (\Delta=\delta/4\pi c) \tag{24a}$$

$$(v_s, l_s, v_{s''}|H_1'/hc|v_s+2, l_s, v_{s''}-1)=(v_s+2, l_s, v_{s''}-1|H_1'/hc|v_s, l_s v_{s''})$$
$$=(-k_{sss''}/2)[(v_s+2)^2-l_s^2]^{\frac{1}{2}}(v_{s''}/2)^{\frac{1}{2}}, \tag{24b}$$

where l_s takes the values $v_s, v_s-2, \cdots 1$, or 0.

As in the preceding example the elements of the transformed second-order Hamiltonian which are diagonal in the quantum numbers are the same as those in Part I, except insofar as those terms which have $k_{sss''}^2$ as coefficients are concerned. These elements contribute only to x_{ss}, $x_{ss''}$, and $x_{l_sl_s}$, and the terms which have $k_{sss''}^2$ as a coefficient are altered from $(-k_{sss''}^2/4\omega_{s''})(8\omega_s^2-3\omega_{s''}^2)/(4\omega_s^2-\omega_{s''}^2)$ to $-k_{sss''}^2[(1/2\omega_{s''})+1/8(2\omega_s+\omega_{s''})]$ in x_{ss}, from $-2k_{sss''}^2\omega_s/(4\omega_s^2-\omega_{s''}^2)$ to $(-k_{sss''}^2/2)/(2\omega_s+\omega_{s''})$ in $x_{ss''}$, and from $(-k_{sss''}^2/4)\omega_{s''}/(4\omega_s^2-\omega_{s''}^2)$ to $(k_{sss''}^2/8)/(2\omega_s+\omega_{s''})$ in $x_{l_sl_s}$. These will be seen to be the same as those occurring in the expressions for x_{ss}, $x_{ss''}$, and $x_{l_sl_s}$ given in Part I, except that the part containing $(2\omega_s-\omega_{s''})$ as a denominator is absent.

The actual energy values may be obtained by diagonalizing the matrix H, and this is readily accomplished by setting its secular determinant (i.e., $|(\tau|H|\tau')-E\delta_{\tau\tau'}|$ where τ comprises all the quantum numbers, vibrational and rotational) equal to zero and solving for the roots. For simplicity we confine ourselves to the energies of the non-rotating molecule.

Study the first example considered. The elements of H are diagonal in all the vibration quantum numbers except v_s, $v_{s'}$, and $v_{s''}$. The zero-order energy (13) no longer depends upon the quantum numbers v_s, $v_{s'}$, and $v_{s''}$ independently, but rather upon $v_s+v_{s''}$ and $v_{s'}+v_{s''}$. There exists, therefore, a degeneracy and the degree of degeneracy is the number of ways $v_s+v_{s''}$ and $v_{s'}+v_{s''}$ can be made to add up to a given value. For example, consider that $v_s+v_{s''}$ and $v_{s'}+v_{s''}$ are made equal to one. This can happen if $v_s=v_{s'}=1$ and $v_{s''}=0$ or if $v_s=v_{s'}=0$ and $v_{s''}=1$. In both cases $(E_0/hc)=2(\omega_s+\omega_{s'})$ and the level is twofold degenerate, and the matrix elements relating to this level form a step matrix of two rows and columns grouped about the principal diagonal. This is illustrated in (25):

	$v_s=v_{s'}=1,\ v_{s''}=0$	$v_s=v_{s'}=0,\ v_{s''}=1$
$v_s=v_{s'}=1$, $v_{s''}=0$	$2(\omega_s+\omega_{s'})+\Delta/2$	$k_{ss's''}/(8)^{\frac{1}{2}}$
$v_s=v_{s'}=0$, $v_{s''}=1$	$k_{ss's''}/(8)^{\frac{1}{2}}$	$2(\omega_s+\omega_{s'})+3\Delta/2$

(25)

[7] These matrix components have been computed by Professor W. H. Shaffer of this University who generously made his computations available to the author. The author wishes to express his appreciation to Professor Shaffer for his kindness.

Similarly, in the second example the elements of H are diagonal in the vibration quantum numbers except v_s and $v_{s''}$. There will, as before, be a degeneracy since the zero-order energies (18) do not depend upon the quantum numbers, v_s and $v_{s''}$, independently, but upon $v_s+2v_{s''}$. The degree of the degeneracy is determined by the number of ways in which $v_s+2v_{s''}$ can be made to add up to a given value. Suppose ω_s is a linear harmonic frequency and that we let $2v_{s''}+v_s$ be equal to four. This may take place in the following ways: $v_{s''}=0$, $v_s=4$; $v_{s''}=1$, $v_s=2$; and $v_{s''}=2$, $v_s=0$. The level $(2v_{s''}+v_s)\omega_s$ is, therefore, threefold degenerate, and the matrix elements relating to this level form a step matrix of three rows and columns grouped about the principal diagonal. This step matrix is illustrated in (26):

	$v_{s''}=0,\ v_s=4$	$v_{s''}=1,\ v_s=2$	$v_{s''}=2,\ v_s=0$
$v_{s''}=0$, $v_s=4$	$(11\omega_s/2)+\Delta/2$	$(k_{sss''}/2)(6)^{\frac{1}{2}}$	0
$v_{s''}=1$, $v_s=2$	$(k_{sss''}/2)(6)^{\frac{1}{2}}$	$(11\omega_s/2)+3\Delta/2$	$(k_{sss''}/2)(2)^{\frac{1}{2}}$
$v_{s''}=2$, $v_s=0$	0	$(k_{sss''}/2)(2)^{\frac{1}{2}}$	$(11\omega_s/2)+5\Delta/2$

(26)

The example where ω_s is a two-dimensionally isotropic frequency has been examined by Dennison[8] and will not be discussed here.

The matrix of the vibration energy will, therefore, to this approximation contain elements along the principal diagonal only, except insofar as v_s, $v_{s'}$, and $v_{s''}$ are concerned. The diagonalization may then be accomplished by diagonalizing each substep independently. When the roots have been evaluated, the stabilized wave functions for the component states may readily be obtained since these will be linear combinations of the wave functions of the unperturbed states, the coefficients multiplying each term being the normalized cofactors of the secular determinant.

III. THE CORIOLIS TYPE RESONANCE INTERACTION

We shall investigate, in this section, a perturbation which arises when two mutually perpendicular vibrations interact with the rotational motion of the molecule through the Coriolis operator:

$$\sum_{ss'} [(\lambda_{s'}/\lambda_s)^{\frac{1}{2}} q_{ss} p_{s's'} - (\lambda_s/\lambda_{s'})^{\frac{1}{2}} q_{s's'} p_{ss}][(\xi_{sss's'} P_x/I_{xx}^{(e)}) + (\eta_{sss's'} P_y/I_{yy}^{(e)}) + (\zeta_{sss's'} P_z/I_{zz}^{(e)})]. \quad (27)$$

The quantities $\xi_{sss's'}$, $\eta_{sss's'}$, and $\zeta_{sss's'}$ which occur in (27) are the Coriolis coupling coefficients and depend in an involved manner upon the nature of the normal coordinates associated with the frequencies ω_s and $\omega_{s'}$. The term (27) may be removed from the first-order Hamiltonian by transforming H using the transformation function:

$$S = -\{[(\lambda_s+\lambda_{s'}) q_{ss} q_{s's'} + 2\lambda_s^{\frac{1}{2}} \lambda_{s'}^{\frac{1}{2}} p_{ss} p_{s's'}/\hbar^2]/\lambda_s^{\frac{1}{2}} \lambda_{s'}^{\frac{1}{2}} (\lambda_s - \lambda_{s'})\}$$
$$\times\{(\xi_{sss's'} P_x/I_{xx}^{(e)}) + (\eta_{sss's'} P_y/I_{yy}^{(e)}) + (\zeta_{sss's'} P_z/I_{zz}^{(e)})\}. \quad (28)$$

The transformation of H by S gives rise to terms in the second-order Hamiltonian with the denominator $(\lambda_s-\lambda_{s'})$, (i.e., $\omega_s-\omega_{s'}$). When $\lambda_s^{\frac{1}{2}}$ is very nearly equal to $\lambda_{s'}^{\frac{1}{2}}$, resonance sets in and we have much the same difficulty as that which arose in the preceding section. In this example it is the $(v_{ss}, v_{s's'} | v_{ss} \pm 1,\ v_{s's'} \mp 1)$ matrix elements of the operator (27) which present difficulty. We may proceed as in Section II to transform H by a contact transformation such that it will have only the elements $(v_{ss}, v_{s's'} | v_{ss} \pm 1, v_{s's'} \mp 1)$, these being the same identically as the corresponding elements of

[8] D. M. Dennison, Rev. Mod. Phys. 12, 175 (1940).

the operator (27). It will be noted that

$$H^{(1)'}_{ss's'\sigma'}=\tfrac{1}{2}\sum_{\sigma\sigma'}[(\lambda_s^{\frac{1}{2}}+\lambda_{s'}^{\frac{1}{2}})/(\lambda_s^{\frac{1}{2}}\lambda_{s'}^{\frac{1}{2}})][q_{s\sigma}p_{s'\sigma'}-q_{s'\sigma'}p_{s\sigma}][(\xi_{ss's'\sigma'}P_x/I_{xx}^{(e)})$$
$$+(\eta_{ss's'\sigma'}P_y/I_{yy}^{(e)})+(\zeta_{ss's'\sigma'}P_z/I_{zz}^{(e)}], \quad (29)$$

satisfies the above requirements. Since S will remove the operator (27) completely from H_1' we may expect to derive the function S^* required by adding to S a function s which will put the expression (29) back into the transformed first-order Hamiltonian H_1'. It may be verified that the correct form for s will be

$$s=\tfrac{1}{2}[(\lambda_s^{\frac{1}{2}}+\lambda_{s'}^{\frac{1}{2}})^2/\lambda_s^{\frac{1}{2}}\lambda_{s'}^{\frac{1}{2}}(\lambda_s-\lambda_{s'})][q_{s\sigma}q_{s'\sigma'}+p_{s\sigma}p_{s'\sigma'}/\hbar^2][(\xi_{ss's'\sigma'}P_x/I_{xx}^{(e)})$$
$$+(\eta_{ss's'\sigma'}P_y/I_{yy}^{(e)})+(\zeta_{ss's'\sigma'}P_z/I_{zz}^{(e)})]. \quad (30)$$

Evidently the transformation function $S^*=S+s$ suitable for our problem will be:

$$S^*=\tfrac{1}{2}[(\lambda_{s'}^{\frac{1}{2}}-\lambda_s^{\frac{1}{2}})/\lambda_s^{\frac{1}{2}}\lambda_{s'}^{\frac{1}{2}}(\lambda_s^{\frac{1}{2}}+\lambda_{s'}^{\frac{1}{2}})][q_{s\sigma}q_{s'\sigma'}-p_{s\sigma}p_{s'\sigma'}/\hbar^2][(\xi_{ss's'\sigma'}P_x/I_{xx}^{(e)})$$
$$+(\eta_{ss's'\sigma'}P_y/I_{yy}^{(e)})+(\zeta_{ss's'\sigma'}P_z/I_{zz}^{(e)})]. \quad (31)$$

It does not contain the denominator $(\lambda_s^{\frac{1}{2}}-\lambda_{s'}^{\frac{1}{2}})$.

Consider now the two frequencies ω_s and $\omega_{s'}$ which are assumed to arise from two linear harmonic oscillations which are perpendicular to each other. We proceed as in Section II by assuming that $\lambda_s^{\frac{1}{2}}\approx\lambda_{s'}^{\frac{1}{2}}$ so that we may write $\lambda_{s'}^{\frac{1}{2}}=\lambda_s^{\frac{1}{2}}+\delta$, δ being a small quantity. The zero-order Hamiltonian pertaining to these two frequencies may be written:

$$H_0=(\hbar\lambda_s^{\frac{1}{2}}/2)[(p_s^2/\hbar^2+q_s^2)+(p_{s'}^2/\hbar^2+q_{s'}^2)], \quad (32)$$

H_0 has the eigenvalue

$$(E_0/hc)=(v_s+v_{s'}+1)\omega_s. \quad (33)$$

The first-order transformed Hamiltonian will be:

$$H_1'=(\delta\hbar/2)(p_{s'}^2/\hbar^2+q_{s'}^2)+H_{ss'}^{(1)}. \quad (34)$$

H_1' has the following non-vanishing matrix components:

$$(\cdots v_s, v_{s'}\cdots K|H_1'/hc|\cdots v_s, v_{s'}\cdots K)=\Delta(v_s+\tfrac{1}{2}), \quad (\Delta=\delta/4\pi c) \quad (35a)$$

$$(\cdots v_s, v_{s'}\cdots K|H_1'/hc|\cdots v_s+1, v_{s'}-1\cdots K)=-(\cdots v_s+1, v_{s'}-1\cdots K|H_1'/hc|\cdots v_s, v_{s'}\cdots K)$$
$$=i\zeta_{ss'}Z_eK[(\lambda_s^{\frac{1}{2}}+\lambda_{s'}^{\frac{1}{2}})/(\lambda_s\lambda_{s'})^{\frac{1}{2}}](v_s+1)^{\frac{1}{2}}(v_{s'})^{\frac{1}{2}}, \quad (35b)$$

$$(\cdots v_s, v_{s'}\cdots K|H_1'/hc|\cdots v_s+1, v_{s'}-1\cdots K\pm1)$$
$$=-(\cdots v_s+1, v_{s'}-1\cdots K|H_1'/hc|\cdots v_s, v_{s'}\cdots K\pm1)$$
$$=\pm\tfrac{1}{2}[\eta_{ss'}Y_e\pm i\xi_{ss'}X_e][J(J+1)-K(K\pm1)]^{\frac{1}{2}}[(\lambda_s^{\frac{1}{2}}+\lambda_{s'}^{\frac{1}{2}})/(\lambda_s\lambda_{s'})^{\frac{1}{2}}](v_s+1)^{\frac{1}{2}}(v_{s'})^{\frac{1}{2}}. \quad (35c)$$

The transformed second-order Hamiltonian H_2' will, of course, also be altered, but only insofar as the coefficients of the operators P_x^2, P_y^2, and P_z^2 are concerned which are multiplied by $\xi_{ss'}^2$, $\eta_{ss'}^2$, and $\zeta_{ss'}^2$. When the contact transformation of H has been completed, the above coefficients will be replaced by

$$[(\hbar/8)(\lambda_s\lambda_{s'})^{\frac{1}{2}}(\lambda_s^{\frac{1}{2}}-\lambda_{s'}^{\frac{1}{2}})/(\lambda_s^{\frac{1}{2}}+\lambda_{s'}^{\frac{1}{2}})]\{[3(\lambda_{s'}/\lambda_s)^{\frac{1}{2}}+(\lambda_s/\lambda_{s'})^{\frac{1}{2}}]q_{s\sigma}^2$$
$$-[(\lambda_{s'}/\lambda_s)^{\frac{1}{2}}+3(\lambda_s/\lambda_{s'})^{\frac{1}{2}}](p_{s\sigma}^2/\hbar^2)\}\{(\xi_{ss'}P_x/I_{xx}^{(e)})+(\eta_{ss'}P_y/I_{yy}^{(e)})+(\zeta_{ss'}P_z/I_{zz}^{(e)})\}^2. \quad (36)$$

To this approximation H_2' will contribute only to the diagonal elements of the matrix H, and these will be exactly the second-order corrections to the reciprocals of inertia given in Part I except that the terms containing $\lambda_s/(\lambda_s-\lambda_{s'})$ which occur in the rotational constants x_{ss}, y_{ss}, and z_{ss} will be absent

	$(\frac{1}{2})^{\frac{1}{2}}\psi(v_s=1, v_{s'}=0)\times(\psi(-1)-\psi(1))$	$(\frac{1}{2})^{\frac{1}{2}}\psi(v_s=0, v_{s'}=1)\times(\psi(-1)+\psi(1))$	$(\frac{1}{2})^{\frac{1}{2}}\psi(v_s=1, v_{s'}=0)\times(\psi(-1)+\psi(1))$	$(\frac{1}{2})^{\frac{1}{2}}\psi(v_s=0, v_{s'}=1)\times(\psi(-1)-\psi(1))$	$\psi(v_s=1, v_{s'}=0)\times\psi(0)$	$\psi(v_s=0, v_{s'}=1)\psi(0)$
$(\frac{1}{2})^{\frac{1}{2}}\psi(v_s=1, v_{s'}=0)\times(\psi(-1)-\psi(1))$	$R_0+R_2+R_3+3\Delta/2-2(R_s+2R_s)-\epsilon$	$iZ_s\xi_{ss'}\times[(\lambda_s^{\frac{1}{2}}+\lambda_{s'}^{\frac{1}{2}})/(\lambda_s\lambda_{s'})^{\frac{1}{2}}]$	0	0	0	0
$(\frac{1}{2})^{\frac{1}{2}}\psi(v_s=0, v_{s'}=1)\times(\psi(-1)+\psi(1))$	$-iZ_s\xi_{ss'}\times[(\lambda_s^{\frac{1}{2}}+\lambda_{s'}^{\frac{1}{2}})/(\lambda_s\lambda_{s'})^{\frac{1}{2}}]$	$R_0'+R_2'+R_3'+\Delta/2-2(R_s'+2R_s')-\epsilon$	0	0	0	0
$(\frac{1}{2})^{\frac{1}{2}}\psi(v_s=1, v_{s'}=0)\times\psi(-1)+\psi(1))$	0	0	$R_0+R_2+R_3+3\Delta/2+2(R_s+2R_s)-\epsilon$	$iZ_s\xi_{ss'}\times[(\lambda_s^{\frac{1}{2}}+\lambda_{s'}^{\frac{1}{2}})/(\lambda_s\lambda_{s'})^{\frac{1}{2}}]$	0	0
$(\frac{1}{2})^{\frac{1}{2}}\psi(v_s=0, v_{s'}=1)\times(\psi(-1)-\psi(1))$	0	0	$-iZ_s\xi_{ss'}\times[(\lambda_s^{\frac{1}{2}}+\lambda_{s'}^{\frac{1}{2}})/(\lambda_s\lambda_{s'})^{\frac{1}{2}}]$	$R_0'+R_2'+R_3'+\Delta/2-2(R_s'+2R_s')-\epsilon$	0	0
$\psi(v_s=1, v_{s'}=0)\psi(0)$	0	0	0	0	$R_0+3\Delta/2-\epsilon$	0
$\psi(v_s=0, v_{s'}=1)\psi(0)$	0	0	0	0	0	$R_0'+\Delta/2-\epsilon$

(38)

and in their place will be found, respectively:

$$\xi_{ss'}{}^2X_s(h/2I_{zz}{}^{(s)}(\lambda_s\lambda_{s'})^{\frac{1}{2}})[(\lambda_s^{\frac{1}{2}}-\lambda_{s'}^{\frac{1}{2}})/(\lambda_s^{\frac{1}{2}}+\lambda_{s'}^{\frac{1}{2}})],$$
$$\eta_{ss'}{}^2Y_s(h/2I_{yy}{}^{(s)}(\lambda_s\lambda_{s'})^{\frac{1}{2}})[(\lambda_s^{\frac{1}{2}}-\lambda_{s'}^{\frac{1}{2}})/(\lambda_s^{\frac{1}{2}}+\lambda_{s'}^{\frac{1}{2}})],$$
$$\zeta_{ss'}{}^2Z_s(h/2I_{zz}{}^{(s)}(\lambda_s\lambda_{s'})^{\frac{1}{2}})[(\lambda_s^{\frac{1}{2}}-\lambda_{s'}^{\frac{1}{2}})/(\lambda_s^{\frac{1}{2}}+\lambda_{s'}^{\frac{1}{2}})]. \quad (37)$$

The energy values themselves are obtained as before by solving for the roots of the secular determinant of the matrix which has the elements (32), (35), and (37). To second order of approximation all the terms are diagonal in the vibration quantum numbers v_s and $v_{s'}$. The zero-order energies are degenerate in the frequencies ω_s and $\omega_{s'}$ since they depend not upon v_s and $v_{s'}$ independently, but upon $v_s+v_{s'}$. The degree of the degeneracy depends upon the number of ways $v_s+v_{s'}$ can be made to add up to the same number. The elements associated with the resonating components form a sub-matrix of the matrix of H. This sub-matrix will contain as many rows and columns as the degree of the degeneracy, its elements being grouped about the principal diagonal of the matrix in a little box. Diagonalization of the matrix is accomplished simply by diagonalizing these sub-matrices by themselves. Once the roots of the secular determinant are known, the stabilized wave functions are immediately available since they are linear combinations of the zero-order wave functions of the component levels, the coefficients of these being the normalized first minors of the secular determinant.

We shall examine the case where the frequencies ω_s and $\omega_{s'}$ lie in the xy plane of the molecule as is the case in the planar ZXY_2 molecular model studied by Silver.[9] This is tantamount to setting $\xi_{ss'}=\eta_{ss'}=0$ in which case the matrix elements $(v_s, v_{s'}, K|v_s\pm1, v_s\mp1, K\pm1)$ will vanish. If we confine ourselves to the fundamental frequencies ω_s and $\omega_{s'}$ (i.e., $v_s=1$, $v_{s'}=0$, and $v_s=0$, $v_{s'}=1$), we have specifically the case described by Silver.[9] We shall set up the secular determinant of the sub-matrix associated with these frequencies for the value of $J=1$, J being the quantum number of total angular momentum. We follow Silver and use as the basic rotational wave functions $(\frac{1}{2})^{\frac{1}{2}}[\psi(K=1)\pm\psi(K=-1)]$ and $\psi(K=0)$ instead of the functions $\psi(K=1)$, $\psi(K=-1)$ and $\psi(K=0)$. We have then Eq. (38) as given in

[9] S. Silver, J. Chem. Phys. 10, 565 (1942).

adjacent column where the R_i are the values of R_i defined in Eq. (27), Part I, where $v_s=1$ and $v_{s'}=0$ and the R_i' are the values when $v_s=0$ and $v_{s'}=1$. The roots of (38) will be seen to be those given by Silver[9] for the state $J=1$.

The selection rules for the quantum number K are altered by this type of resonance interaction. This question has been dealt with elsewhere[10] and need not be repeated here.

Another example, which may be regarded as a generalization of the previous example, but which is sufficiently different from the foregoing to warrant separate mention, is the one where there are three resonating frequencies, ω_s, $\omega_{s'}$, and $\omega_{s''}$ (i.e., $\lambda_{s'}^{\frac{1}{2}}=\lambda_s^{\frac{1}{2}}+\delta$ and $\lambda_{s''}^{\frac{1}{2}}=\lambda_s^{\frac{1}{2}}+\delta'$, δ and δ' being small quantities), arising from three linear harmonic oscillations which are mutually perpendicular to each other. We shall confine ourselves to the situation where the vibrations associated with the frequencies ω_s, $\omega_{s'}$, and $\omega_{s''}$ are respectively along the body fixed axes z, x, and y. This is equivalent to declaring that only the Coriolis coupling factors, $\xi_{s's}$, $\eta_{ss''}$, and $\zeta_{s''s'}$, are different from zero. In this case there will be matrix elements of all the types given in (35) which are non-vanishing. We shall here consider only the fundamental frequencies, ω_s, $\omega_{s'}$, and $\omega_{s''}$ (i.e., $v_s=1, v_{s'}=v_{s''}=0$; $v_s=v_{s''}=0$, $v_{s'}=1$; $v_s=v_{s'}=0$, $v_{s''}=1$), and set up the secular determinant for the sub-matrix associated with these frequencies for the value of $J=1$, J being the quantum number of total angular momentum. We follow a method

	$F\,R(1)$	$G\,R(0)$	$H\,R(-1)$	$F\,R(0)$	$G\,R(-1)$	$G\,R(1)$	$H\,R(0)$	$F\,R(-1)$	$H\,R(1)$
$F\,R(1)$	$\frac{1}{2}(R_{aa}+R_{ss}+R_{ss}+R_{ss}+R_{ss})-2\zeta Z_e-\epsilon$	α	0	0	0	0	0	β	$\frac{1}{2}(R_{aa}+R_{ss}+R_{ss}-R_{ss}-R_{ss})$
$G\,R(0)$	α	$R_{ee}-\epsilon$	$-\alpha$	0	0	0	0	γ	$-\gamma$
$H\,R(-1)$	0	$-\alpha$	$\frac{1}{2}(R_{aa}+R_{ss}+R_{ss}+R_{ss}+R_{ss})-2\zeta Z_e-\epsilon$	0	0	0	0	$\frac{1}{2}(R_{aa}+R_{ss}+R_{ss}-R_{ss}-R_{ss})$	β
$F\,R(0)$	0	0	0	$\frac{1}{2}(R_{aa}+R_{ss})-\epsilon$	α	γ	$\frac{1}{2}(R_{aa}-R_{ss})$	0	0
$G\,R(-1)$	0	0	0	α	$(R_{cc}+R_{zz}+R_{xx})-\epsilon$	β	$-\gamma$	0	0
$G\,R(1)$	0	0	0	γ	β	$(R_{ee}+R_{zz}+R_{xx})-\epsilon$	$-\alpha$	0	0
$H\,R(0)$	0	0	0	$\frac{1}{2}(R_{aa}-R_{ss})$	$-\gamma$	$-\alpha$	$\frac{1}{2}(R_{aa}+R_{ss})-\epsilon$	0	0
$F\,R(-1)$	β	γ	$\frac{1}{2}(R_{aa}+R_{ss}+R_{ss}-R_{ss}-R_{ss})$	0	0	0	0	$\frac{1}{2}(R_{aa}+R_{ss}+R_{ss}+R_{ss}+R_{ss})+2\zeta Z_e-\epsilon$	0
$H\,R(1)$	$\frac{1}{2}(R_{aa}+R_{ss}+R_{ss}-R_{ss}-R_{ss})$	$-\gamma$	β	0	0	0	0	0	$\frac{1}{2}(R_{aa}+R_{ss}+R_{ss}+R_{ss}+R_{ss})+2\zeta Z_e-\epsilon$

(39)

[10] H. H. Nielsen, J. Chem. Phys. 5, 818 (1937).

suggested by the work of Shaffer, Nielsen, and Thomas[3] and use as the basic wave functions the following: $FR(K)$, $GR(K)$, and $HR(K)$, F and H being, respectively, $(\frac{1}{2})^{\frac{1}{2}}\begin{pmatrix} {}^{1}_{0}\varphi & {}^{0}_{0} \\ {}^{0}_{0}\varphi \pm i\,{}^{1}_{0}\varphi & {}^{0}_{0} \end{pmatrix}$ and $G={}^{0}_{1}\varphi$ where ${}^{1}_{0}\varphi=\psi(v_a=0, v_{a'}=0, v_{a''}=1)$ ${}^{0}_{0}\varphi=\psi(v_a=0, v_{a'}=1, v_{a''}=0)$ and ${}^{0}_{1}\varphi=\psi(v_a=1, v_{a'}=0, v_{a''}=0)$. In the above functions $R(K)$ is the rotational wave function which for a given J value is characterized by the quantum number K. We have then the rather complicated secular determinant[11] given in Eq. (39) on page 189, where

$$\begin{aligned}
\zeta&=(\zeta_{a''a'}/2)[(\lambda_{a'}^{\frac{1}{2}}+\lambda_{a''}^{\frac{1}{2}})/(\lambda_{a'}\lambda_{a''})^{\frac{1}{2}}],\\
\alpha&=(\xi_{a'a}/2)[(\lambda_a^{\frac{1}{2}}+\lambda_{a'}^{\frac{1}{2}})/(\lambda_a\lambda_{a'})^{\frac{1}{2}}]X_e+(\eta_{aa''}/2)[(\lambda_a^{\frac{1}{2}}+\lambda_{a''}^{\frac{1}{2}})/(\lambda_a\lambda_{a''})^{\frac{1}{2}}]Y_e,\\
\beta&=(1/4)\{[Y(v_{a''}=1)+Y(v_{a'}=1)]-[X(v''=1)+X(v_{a'}=1)]\},\\
\gamma&=(\xi_{a'a}/2)[(\lambda_a^{\frac{1}{2}}+\lambda_{a'}^{\frac{1}{2}})/(\lambda_a\lambda_{a'})^{\frac{1}{2}}]X_e-(\eta_{aa''}/2)[(\lambda_a^{\frac{1}{2}}+\lambda_{a''}^{\frac{1}{2}})/(\lambda_a\lambda_{a''})^{\frac{1}{2}}]Y_e,
\end{aligned} \tag{40}$$

and the R_i's are defined as before.

When the molecule is a symmetric molecule, the reciprocals of inertia X_v and Y_v are alike, the frequencies $\omega_{a'}$ and $\omega_{a''}$ are the same (i.e., $\lambda_{a'}^{\frac{1}{2}}=\lambda_{a''}^{\frac{1}{2}}$), and $\xi_{a'a}$ and $\eta_{a''a}$ become equal to each other. The determinant (39) is then much simplified since β and γ reduce to zero and the R_{ia} become respectively equal to the R_{ib}. It will then be seen that the secular determinant factors into five sub-determinants, two identical ones with a single element, two other identical steps with two rows and columns each, and another with three rows and columns. The general secular determinant for a given value of J will have $3(2J+1)$ rows and columns, but will again factor into sub-determinants. There will always be two identical steps with a single element each, two identical steps each with two rows and columns, and the rest will have three rows and columns each. The general form for the sub-determinant will be:

	$FR(K+1)$	$GR(K)$	$HR(K-1)$
$FR(K+1)$	$R_0+(K+1)^2R_2+(K+1)^4R_3-2\zeta(K+1)Z_e-\epsilon$	$\left[\frac{f-K(K+1)}{2}\right]^{\frac{1}{2}}\alpha$	0
$GR(K)$	$\left[\frac{f-K(K+1)}{2}\right]^{\frac{1}{2}}\alpha$	$R_{0e}+K^2R_{2e}+K^4R_3-\epsilon$	$-\left[\frac{f-K(K-1)}{2}\right]^{\frac{1}{2}}\alpha$
$HR(K-1)$	0	$-\left[\frac{f-K(K-1)}{2}\right]^{\frac{1}{2}}\alpha$	$R_0+(K-1)^2R_2+(K-1)^4R_3+2\zeta(K-1)Z_e-\epsilon$

$=0.$ (41)

There will be an odd number of steps with three rows and columns each, and these will be identical in pairs except for the step where $K=0$. In the limiting case of molecules like CH_4 where $X_e=Y_e=Z_e$, the frequencies ω_a, $\omega_{a'}$, and $\omega_{a''}$ form a triply degenerate frequency. It may be shown that $\xi_{a'a}=\eta_{aa''}=\zeta_{a''a}=\zeta$. If the centrifugal distortion term R_3 is neglected in the sub-determinant (41), it yields $(\epsilon-R_0)/hc=2J\zeta B_e$, $(\epsilon-R_0)/hc=-2\zeta B_e$, and $(\epsilon-R_0)/hc=-2(J+1)\zeta B_e$ as the values for the roots. These are the well-known values given by several authors.[12]

It is not practicable here to discuss the selection rules which result because of the resonance since they become quite complicated. One may visualize them somewhat in the following manner. The

[11] The elements $(FR(1)|HR(-1))$, $(HR(-1)|FR(1))$, $(FR(-1)|HR(1))$, and $(HR(1)|FR(-1))$ are not exactly zero as indicated in (39). They are of the order of differences in the anharmonic corrections to the reciprocals of inertia and will, therefore, not contribute to the energy of the molecule in this approximation.

[12] M. Johnston and D. M. Dennison, Phys. Rev. **48**, 868 (1935). H. A. Jahn, Proc. Roy. Soc. **A168**, 469 (1938).

frequencies $\omega_{s'}$ and $\omega_{s''}$ were assumed to lie in the xy plane of the molecule while the frequency ω_s was taken to be along the body fixed axis z. When the molecule is a symmetric molecule and $\omega_{s'}=\omega_{s''}$, we have a twofold degenerate frequency in a plane perpendicular to the axis of symmetry. Such a frequency is termed a perpendicular vibration and the selection rules in the unperturbed case are $\Delta J=\pm 1, 0$; $\Delta K=\pm 1$. The frequency ω_s is non-degenerate and along the axis of symmetry. It is known as a parallel vibration and in the unperturbed case, the selection rules are $\Delta J=\pm 1, 0$; $\Delta K=0$. When resonance sets in there will be a mixing of the wave functions, i.e., the wave functions of the component levels become linear combinations of the unperturbed wave functions. Thus, in the case discussed here, the actual wave functions will be linear combinations of $F\,R(K+1)$, $G\,R(K)$, and $H\,R(K-1)$. This will mean that when a transition takes place from the normal state to the component level which corresponds more nearly to the unperturbed state, ω_s, the resulting spectrum will, to be sure, have the characteristics of a parallel type band, but at the same time it will also possess characteristics of a perpendicular band. In the same manner when a transition occurs from the normal state to the component level $\omega_{s'}(=\omega_{s''})$ the spectrum will have characteristics not only of a perpendicular band, but also to some extent the characteristics of a parallel type band.

By way of conclusion it is perhaps worth while to point out the similarities and the differences between the method here employed to obtain the vibration-rotation energies when vibration frequencies are accidentally degenerate and the method used by Dennison[13] in his study of the carbon dioxide molecule. The method of Dennison is to evaluate the energy matrix by using the zero-order wave functions, i.e., the solutions to the zero-order wave equation. This matrix will, to the desired approximation, have diagonal elements containing zero- and second-order contributions and non-diagonal elements of first- and second-order magnitude. This matrix is then transformed into another matrix which has no off diagonal elements of less than second-order magnitude. To second order of approximation the elements along the principal diagonal may be regarded as the energies of the molecule. When two vibration frequencies, ω_s and $\tau\omega_{s'}$ are close together, the method may fail since the transformed matrix will have second-order correction terms on the principal diagonal which have the denominators $\omega_s-\tau\omega_{s'}$. In such instances where $\omega_s\approx\tau\omega_{s'}$ the elements which cause trouble are the same as those referred to in earlier sections. These are computed on the basis that the energies E_s and $E_{s'}$ are degenerate, and the corresponding elements will be contained in sub-matrices grouped about the principal diagonal. The remaining elements are computed as before, the elements along the principal diagonal being the same, according to Dennison, except that all terms containing the vanishing denominators will be absent.

In our method it is the Hamiltonian which is transformed in such a manner that the first-order Hamiltonian, H_1', vanishes to second order of approximation so that the second-order corrections to the energy are simply the diagonal elements of H_2', and consequently the energies of the molecule may be taken to be just the diagonal elements of $H_0+\epsilon^2H_2'$. When resonance occurs the transformation is of such a character that the first-order Hamiltonian, H_1', while it does not vanish, contains only terms which would give rise to energy corrections that have vanishing denominators. As in Dennison's method their contributions are determined by degenerate perturbation theory, and the elements may be arranged about the principal diagonal in little boxes. It is readily verified by this method that the diagonal elements are exactly the same as when no resonance exists except that they contain no contribution with vanishing denominators.

The author wishes to acknowledge his indebtedness to Dr. Samuel Silver of the Radiation Laboratory at the Massachusetts Institute of Technology who has read this manuscript and verified many of the relations included in it.

[13] D. M. Dennison, Rev. Mod. Phys. 12, 175 (1940).